NSA 15-32927

Pearson

NAA-SR-4515

COPY 29

METALLURGICAL ASPECTS OF SRE FUEL ELEMENT DAMAGE EPISODE

AEC Research and Development Report

ATOMICS INTERNATIONAL

A DIVISION OF NORTH AMERICAN AVIATION, INC.

Price $1.00
Available from the Office of Technical Services
Department of Commerce
Washington 25, D. C.

NSA 15-32937

NAA-SR-4515
METALS, CERAMICS,
AND MATERIALS
46 PAGES

METALLURGICAL ASPECTS OF SRE FUEL ELEMENT DAMAGE EPISODE

By
J. L. BALLIF

ATOMICS INTERNATIONAL

A DIVISION OF NORTH AMERICAN AVIATION, INC.
P.O. BOX 309 CANOGA PARK, CALIFORNIA

AEC
CONTRACT: AT(11-1)-GEN-8
ISSUED: OCT 15 1961

DISTRIBUTION

This report has been distributed according to the category "Metals, Ceramics, and Materials" as given in "Standard Distribution Lists for Unclassified Scientific and Technical Reports" TID-4500 (16th Ed.), December 15, 1960. A total of 620 copies was printed.

ACKNOWLEDGMENT

The work of the Hot Cell Unit of the Fuel Element Development Group, particularly Messrs J.M. Davis and J.F. Leirich and their co-workers, is gratefully acknowledged. Without their cooperation and assistance, this work would not have been possible.

CONTENTS

TABLES

FIGURES

ABSTRACT

An investigation of the metallurgical aspects of the SRE fuel element episode, that occurred July 26, 1959, has been completed. A total of ten hot cell examinations and two special tests were made, with both damaged and undamaged fuel elements from the reactor, ~~to~~ were examin in the hot cell. to determine causative factors. The results show that iron-uranium alloy melting was present. The fuel element channel examined contained ample carbonaceous and/or oxide residue to block the coolant flow, either intemittently or on a permanent basis. Evidence of rapid thermal cycling of the fuel element through the alpha-beta transformation temperature is presented, and is suggested as a second mode of fuel element damage. Investigation of the cladding and structural materials indicated that no damage had occurred from either carburization or from nitriding.

I. INTRODUCTION

During the course of Power Run 14 on the Sodium Reactor Experiment (SRE) at low power, the temperature difference among various fuel channels was found to be undesirably high. Normal operating practices did not succeed in reducing this temperature difference to acceptable values; and, on July 26, 1959, the run was terminated. A series of fuel element inspections was begun, to ascertain the cause of these circumstances. A total of 13 fuel elements were discovered to have suffered substantial damage.

This is the final report on the metallurgical aspects of the SRE Fuel Element Damage Investigation. A previous report[1] was issued, after certain limited investigative work had been carried out. This report will summarize and present all of the work carried on, during this past year and a half, in an attempt to determine the mechanism of the damage to the SRE fuel elements.

Because of the problems encountered in evaluation of the damage and reactor condition, the examination of the fuel elements has required more than a year to complete. It has included ten hot cell examinations and several special tests, in an attempt to duplicate certain of the damage conditions external to the reactor. The investigation was limited to the very minimum necessary to demonstrate the cause and to incorporate suggestions that would eliminate, or at least forstall, this type of happening in the future.

A. REACTOR DESCRIPTION

The following are brief descriptions of the SRE, with respect to the systems pertinent to an understanding of the metallurgical aspects of the problem. The SRE was designed and constructed by Atomics International, a Division of North American Aviation, Inc., as part of a joint program with the Atomic Energy Commission to develop a sodium cooled, graphite moderated, thermal power reactor for civilian application. The Southern California Edison Company installed and is operating the steam electric power generating plant which utilizes heat from the SRE.

The SRE is a thermal reactor, designed as a flexible developmental facility. The reactor was built as a development tool, with emphasis on the investigation of fuel materials. The sodium systems incorporate the use of conventional equipment to the maximum.

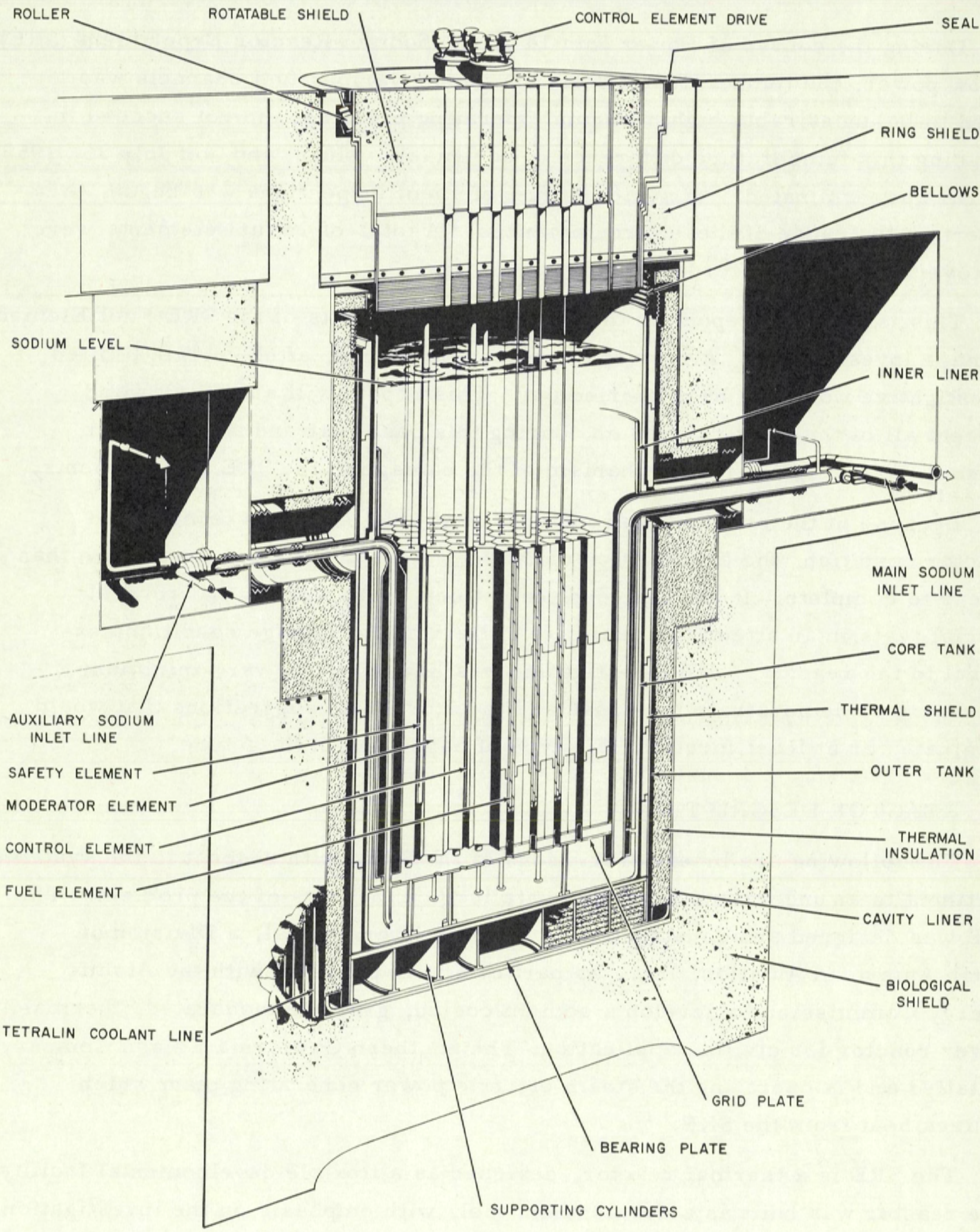

Figure 1. Cross Section of the Reactor

The reactor, Figure 1, is cooled by liquid sodium in the primary loop. Induced Na^{24} activity in the primary loop introduces the need for an intermediate heat exchanger, in which reactor heat is transferred to the secondary loop containing nonradioactive sodium. The secondary system can dissipate reactor heat, either in an airblast heat exchanger or in the steam generator of the Southern California Edison Company's installation. The steam generator is normally used.

1. Irradiation Conditions

The operating conditions of the SRE are shown in Table I. The majority of the core burnup represented in this evaluation took place at or near these conditions. Figure 2 shows the layout of the core face. The center channel and the channels in the first ring have the highest power output.

These fuel channels are used for standard elements that are to be evaluated, and for experimental fuel elements containing thermocouples which read center fuel temperatures at varying distances into the reactor core. The temperature profile can also be calculated from channel power and sodium temperature data. Figure 3 compares the calculated with the measured fuel temperature in the center channel and the first ring channels of the SRE at a power of 20 Mwt. Records are kept of the cumulative thermal power history of the reactor fuel. Figure 4 represents the reactor power and fuel temperature conditions during a typical SRE power run, prior to Runs No. 13 and 14.

2. Coolant

The reactor coolant flow is single pass, with sodium flowing up through the core and collecting above it in a top pool. Over the top pool, a blanket of helium gas is maintained at approximately 3 psig. Circulating pumps draw heated sodium from the reactor top pool and force it through the heat transfer system. The system pressure drop is about 15 psig, at a rated flow of 1080 gpm.

High temperature characteristics of sodium are exploited by utilizing a ΔT of about 450°F across the reactor. The design sodium outlet temperature is 960°F.

TABLE I

SRE CONDITIONS

Type	Thermal Heterogeneous
Capacity	20 Mwt
Moderator	Graphite
Coolant	Sodium T_{in} = 525°F (actual) T_{out} = 950°F (actual) Flow = 800 to 1200 gpm
Fuel Loading	Core I 2.78% Enriched (U^{235}) Unalloyed Uranium Weight - 3000 kg
Fuel Element	No. of Elements - 43 Rods/Element - 7 Overall Length - 8 ft 6 in. Active Length - 6 ft
Flux	Core I Max. thermal neutron flux density - 1.5×10^{13} nv Average thermal neutron flux density - 1.0×10^{13} nv Cell spacing 11 in. on triangular lattice array

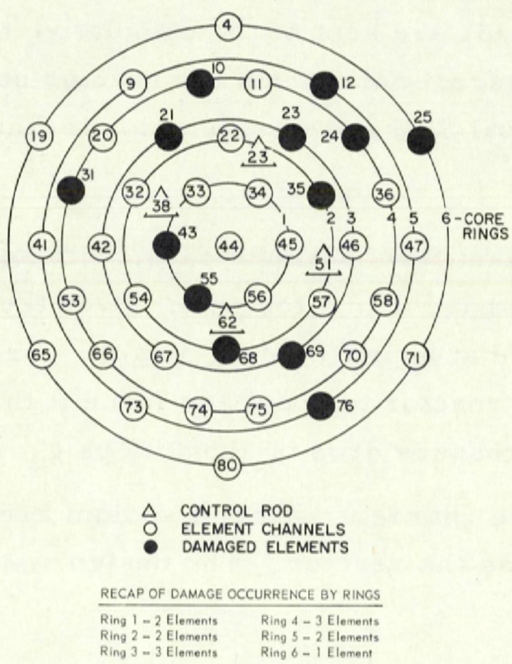

Figure 2. Reactor Face Layout, Locating Damaged Elements

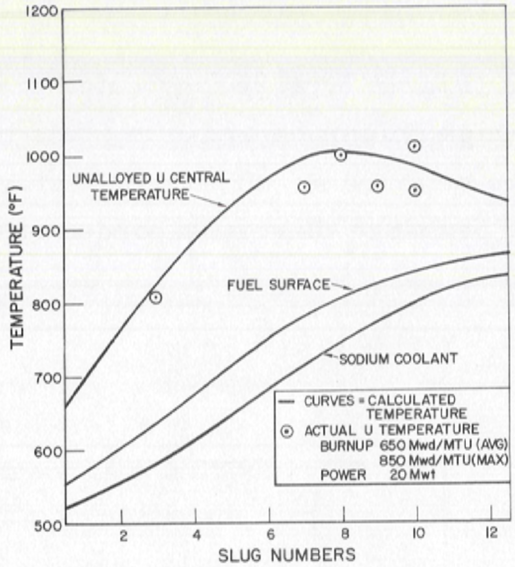

Figure 3. Comparison of Calculated
and Observed Fuel Temperatures

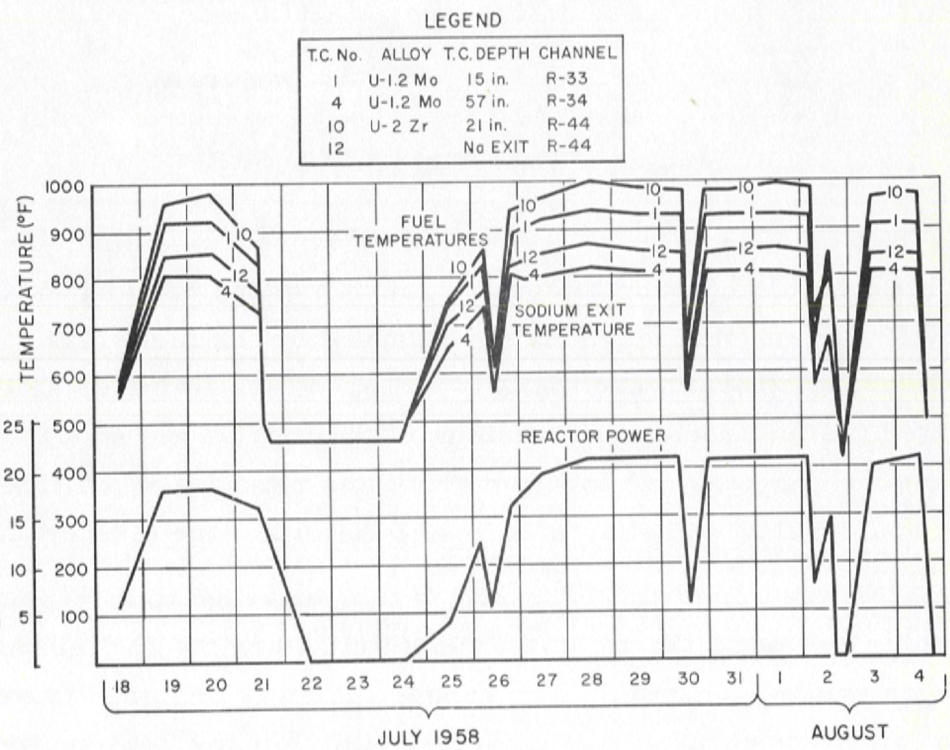

Figure 4. Reactor Power and Temperature
Conditions During a Typical Power Run

3. Fuel Elements

The fuel elements (Figure 5) were fabricated in clusters of seven rods, each consisting of a 6-ft high column of uranium slugs in a thin walled (0.010 in.) stainless steel jacket tube or cladding. The twelve slugs were 0.750 in. in diameter and 6 in. long. They were thermally bonded to the jacket or cladding by

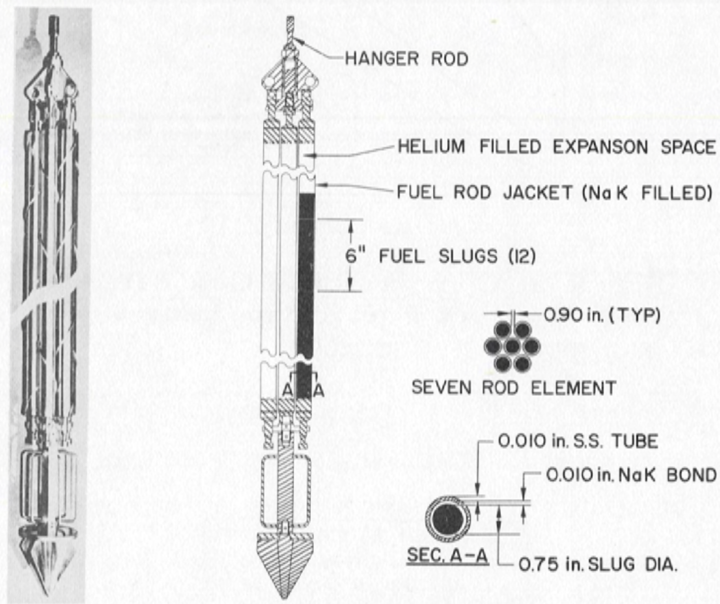

Figure 5. Fuel Element for SRE

a 0.010-in. NaK annulus. Above the column of slugs was a space containing helium. This gas-filled space allowed expansion of the bonding NaK, and served as a reservoir for any fission gases not retained by the fuel slugs. The six outside rods of the cluster were spirally wrapped with stainless steel wire; this prevented the fuel rods from touching each other or the process channel within the moderator cans. A location guide and replaceable orifice plate for controlling sodium flow were fastened to the bottom of the cluster assembly.

The cluster was supported by a hanger tube attached to a stepped shield plug. The shield plug rested in the rotatable top shield when the fuel element was inserted in its process channel. The hanger tube was designed to serve as a holddown for the moderator cans if they should, for any reason, tend to rise in the core. The tube had twelve 3/4-in. diameter drain holes cut in the wall, and six 5/8-in. diameter holes in the end plate, to assure sodium drainage when the element was lifted. A thermocouple indicated the temperature of the sodium at the outlet from the fuel channel. The lead wires passed up the center of the hanger tube. The locations of fuel elements in the core are shown in Figure 3.

During normal operation, there was a pressure drop of about 2.5 psi across the central fuel element, including 1.5 psi across the orifice plate. The design flow of sodium past the central fuel element was 17,500 lb/hr, at a velocity of 5 ft/sec. Outer fuel clusters were orificed to pass lesser amounts of sodium, in accordance with radial power generation distributions within the core. This maintained approximately equal temperatures of the sodium discharge from each process channel into the top sodium pool.

The SRE core was designed for a fuel loading of 37 seven-rod fuel elements. The seven-rod element was designed to provide adequate heat transfer surface to limit the center fuel temperature to 1200°F when the SRE was operating at 20 Mwt.

The metal procurement and fabrication of the α-rolled, β-heat treated uranium are covered in detail in NAA-SR-3456,[2] so these will not be discussed here, except to indicate that every effort was made to process the metal with the best practice available; and that detailed records were kept on all phases of fabrication, from reduction of UF_6 to final assembly of the fuel elements. Each fuel slug in the SRE can be traced to a detailed chemical analysis and a set of fabrication conditions.

B. FUEL ELEMENT EXAMINATION

The examination of the fuel elements, after Run No. 14, was of two types: (1) nondestructive, and (2) destructive. Below are descriptions of the procedures followed in each method.

1. Nondestructive Examination

A special remote technique was developed for viewing fuel elements within the reactor face, using a television camera mounted in the shield plug adapter ring. The elements are raised by the cask hoist and viewed as required. The operators are able to detect any gross cladding defects or mechanical abnormalities by remote viewing. Figure 6 shows the schematic arrangement of the apparatus. This technique has proved useful in checking fuel elements suspected of being grossly defective.

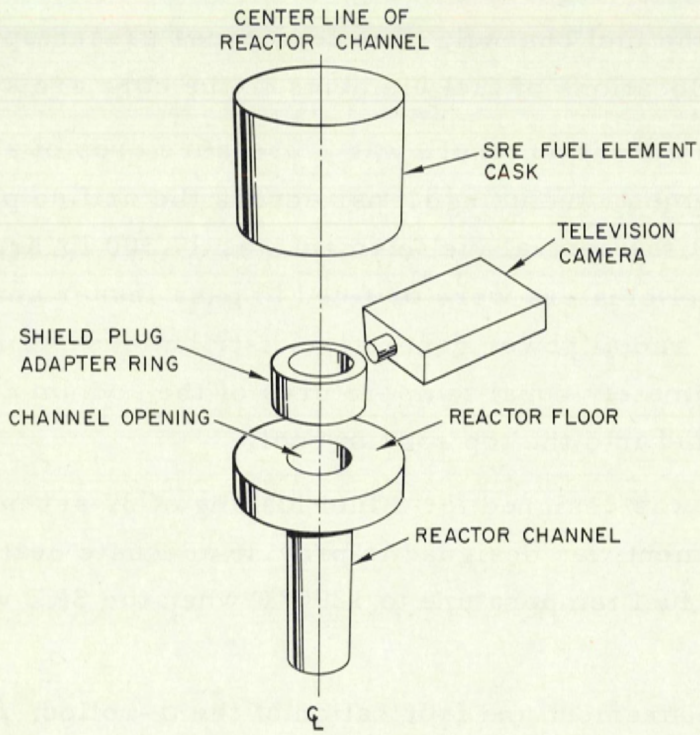

Figure 6. Schematic Arangement for TV Viewing of Fuel Elements

The more detailed nondestructive examination consisted of the following, in a hot cell:

a) Snap gauging for cladding diameter measurement

b) Visual observation for gross abnormalities and/or cladding integrity

The elements selected were examined after each reactor shutdown. Generally, this was the periodic test of the fuel element, to determine external indications of the internal swelling or growth.

The straightness was determined by viewing the fuel element, in a vertical position, with a surveyor's transit in the SRE hot cell. The snap gauging operation, a measurement of outside fuel cladding diameter, was accomplished by a set of snap gauges, actuated in-cell by a master-slave manipulator. The gauging took place on the elements on the side located nearest the reactor center. Thus, with each examination, three rods were gauged, starting from the top of the element rod, every 10 in. down the rod. The element rods required some physical separation, in order for the gauge to slip over the tube. The visual examination consisted of the observation of the fuel element with a 10 power telescope, with field glasses through the shielded glass window, and with magnifying glasses located in the cell.

2. Destructive Examination

The destructive examination consisted of the following, after transporting from the SRE to CDHC:

a) Disassembly of element and decanning of fuel slugs

b) Visual and photographic examination of slugs

c) Dimensional measurement for length, diameter, and warp of slugs

d) Surface measurement of slugs

e) Density determination of slugs

f) Burnup analysis, by gamma-radiation detection techniques and radiochemical analysis of slug specimens

g) Metallographic examination of slugs and cladding

Generally, examinations required (a) the cleaning of the elements in an alcohol bath, since none of the elements had been washed, (b) the disassembly of the fuel cluster, then (c) the decanning of the fuel rod, to allow measurement of each individual fuel slug. Each slug was considered as a unit, and had a corresponding temperature and burnup associated with it. After the opening of the rod, the NaK bond material, where present, was digested in an alcohol-kerosene solution. The individual slugs were cleaned and stored under kerosene in the cell. After decanning and cleaning, visual examination and photography were completed, to show surface variation and any gross defect. Each slug was given a thorough visual examination, both with the unaided eye and with a 10 power telescope. Dimensional measurements were then taken. Diameters were read at five equispaced points, then the slug was rotated 90° and the measurements were repeated. Three length measurements were made, one on the central axis and two at opposite points on the circumference. The density measurements, using the Archimedes method, were carried out on a direct-weighing balance, adapted for remote operation.

An experimental setup was in use to read gamma-ray intensity for determining relative burnup of individual slugs from the fuel rod. The slug was centered in the hot cell, in front of a 1/8-in. diameter hole running through the shielded wall. A scintillation detector was located at the other end of the hole, and operated a gamma spectrometer, set to record only gamma-ray energies in excess of 700 kev. However, this provided only relative information; and thus a radiochemical burnup determination was necessary, to convert the data from gamma scanning to absolute burnup figures.

Sections from the representative slugs were taken for hot metallographic examinations. These were examined for structure, gas voids, and any apparent damage or abnormality.

C. CHEMICAL ANALYSIS

Chemical samples were secured from the defective elements and the materials associated with them. This was for the purpose of determining the presence of eutectic and position within the debris that was recovered. However, most of the material recovered was too radioactive to be handled in the existing facilities. The same was true with the hot cell metallography.

D. HANDLING

Several problems were encountered in this investigation, relative to the handling of the fuel elements. Because of the nature of the damage, found during the observation of the elements in the fuel handling cask, it was decided that washing of the element (or any exposure longer than a few moments) was taking undue risk as to fire or other associated hazards. For this reason, the procedure for handling of the elements was modified from that normally used. It included the observation of each element, through the fuel handling cask periscope, as the element was lifted from the reactor channel position, to determine whether it was intact. Those that were judged acceptable were moved into the storage cells. Those that were damaged were handled in the SRE Hot Cell, by lowering them through the roof port into an argon-filled Pyrex glass encasement. This allowed the element to be more thoroughly viewed, as it dropped into the cell for placement in the fuel element storage can. These cans were made from Type 304 stainless steel tubes, about 4 in. in diameter, with welded plates on their lower ends, and screw-on tops. They also had spring bumper plates in the bottom, in order to reduce stresses in the element from resulting dropping to the bottom of the cask. As the element was lowered into the cell, the bottom section of the Pyrex glass enclosure was raised, to facilitate the movement of a hydraulically operated shear which cut the hanger rod, thereby dropping the element into the storage can. Before screwing the top on, the can was purged and filled with argon. The loaded cans were then stored in the radioactive waste disposal area.

The SRE Hot Cell is only equipped to change orifice plates and carry out light maintenance work on the fuel elements. Therefore, the detailed examination of the elements took place in the general purpose Component Development Hot Cell. This necessitated the transporting of the fuel element in a special cask mounted on a truck and trailer.

II. RESULTS

The results of this investigation are presented as figures, because the greatest part of the evidence presented is of a pictorial nature. However, a brief summary of these results follows:

A. Evidence of low temperature alloy formation or eutectic melting

1. Fuel Element R-55, showing adhering eutectic (Figure 7)

2. Fuel Element R-24, showing melted area and fuel "blob" (Figure 8)

B. Evidence of plugging or blocking of fuel channel

1. The "goo" found on Fuel Element R-55 (Figure 7)

2. The plugged section beneath the orifice R-24 (Figure 8)

C. Evidence of thermal cycling, as a cause for failure

1. Fuel Element R-24 (Figure 8)

2. Fuel Element R-25 (Figure 9)

3. Fuel Element R-21 (Figures 10 and 11)

4. Thermal cycling data (Figure 12)

5. Examples of failures from out-of-pile tests (Figure 9)

D. Metallographic evidence of the absence of structural damage on fuel element components (Figure 13)

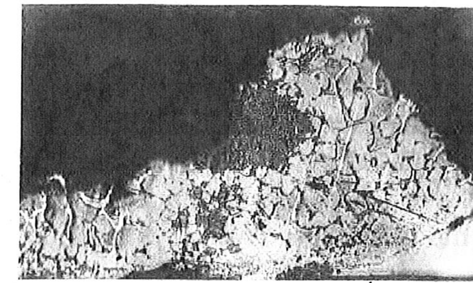

e. 43X

f. 300X

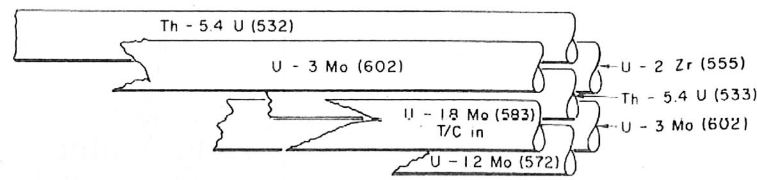

d.

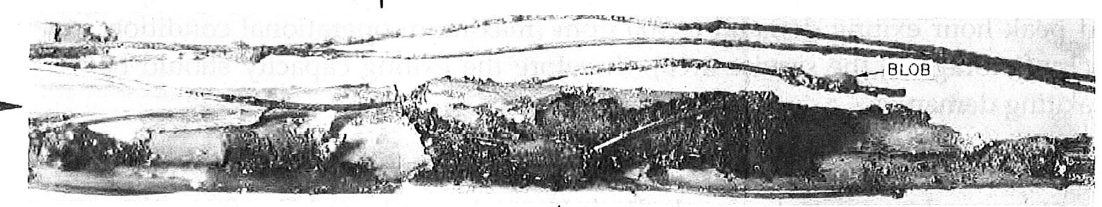

c.

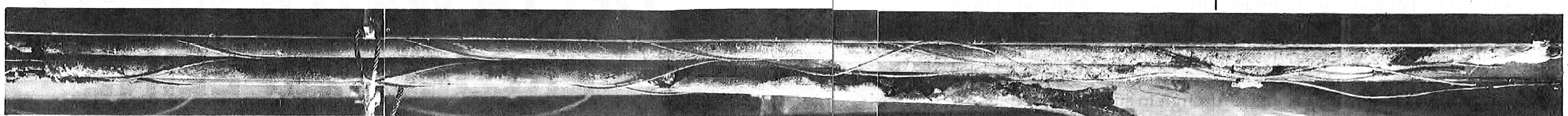

a. Composite of Fuel Eleme SU-2-5 (R-55)

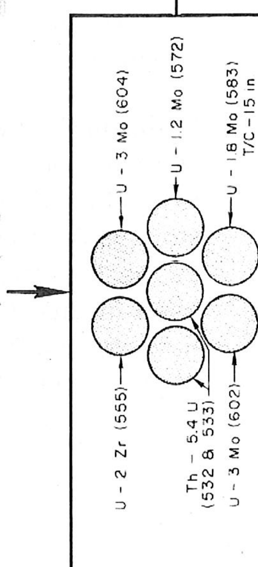

h.

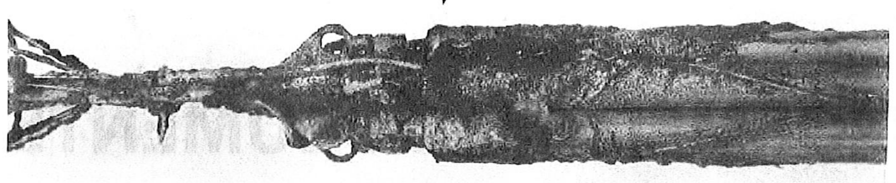

b. Residue Found on Top of Element

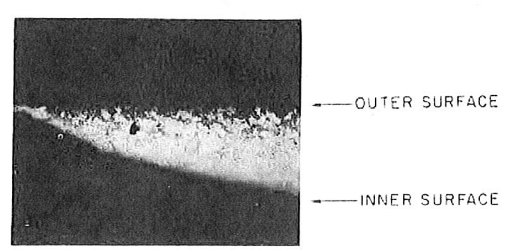

(1) 45X

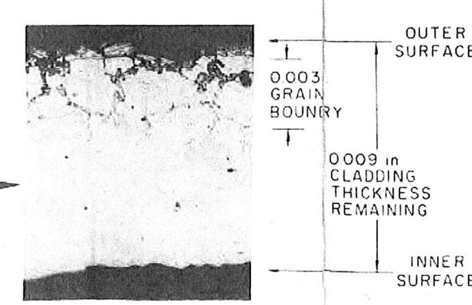

(2) 115X

g. Sections of Cladding Adjacent to Melted Area

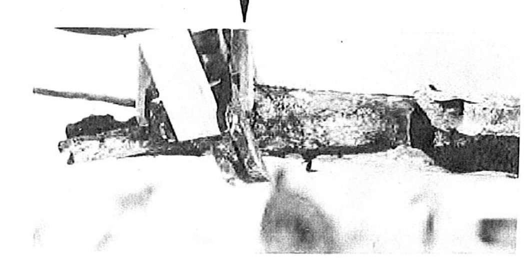

FIGURE 7 LEFT

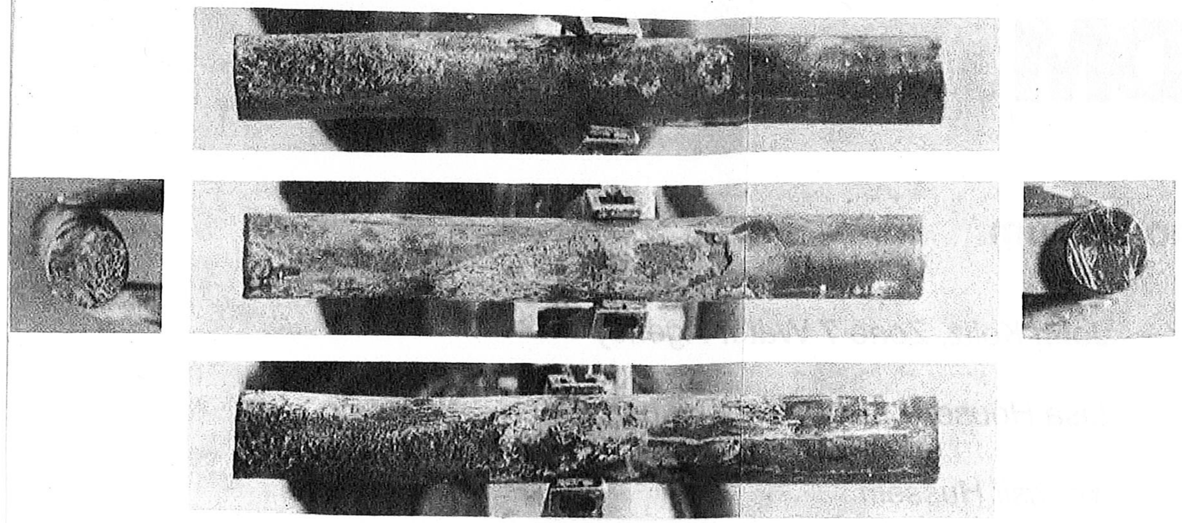

j. U - 1.2 Mo (572)

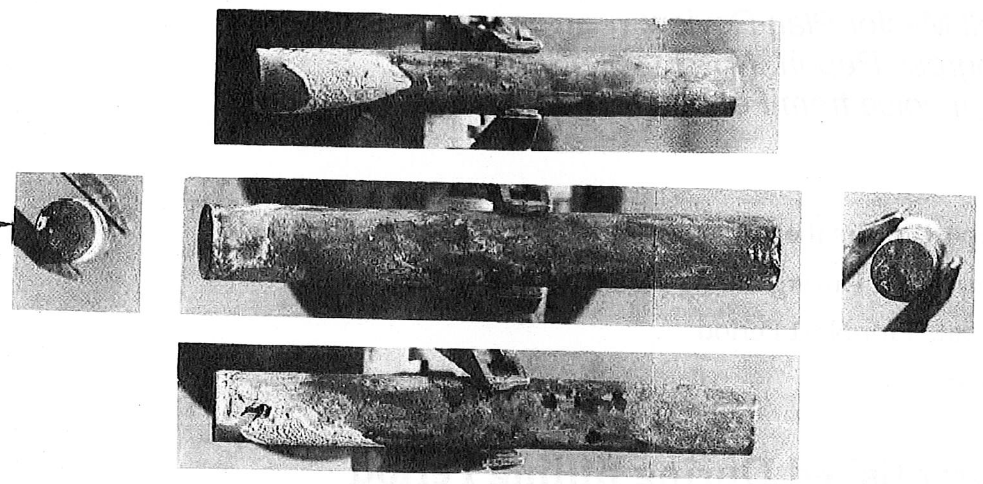

k. U - 3 Mo (602)

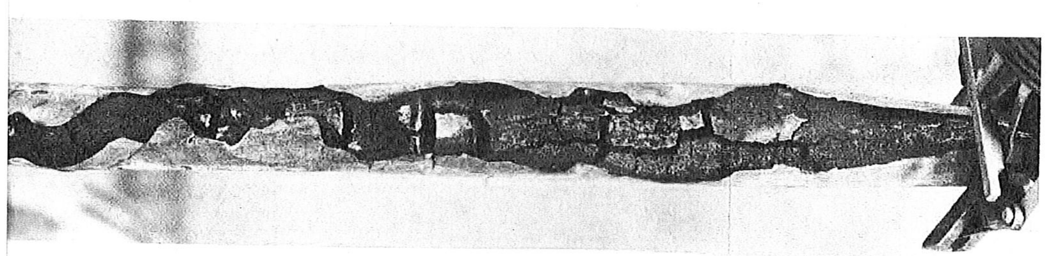

i. U – 2 Zr (555)

FIGURE 7 CENTER

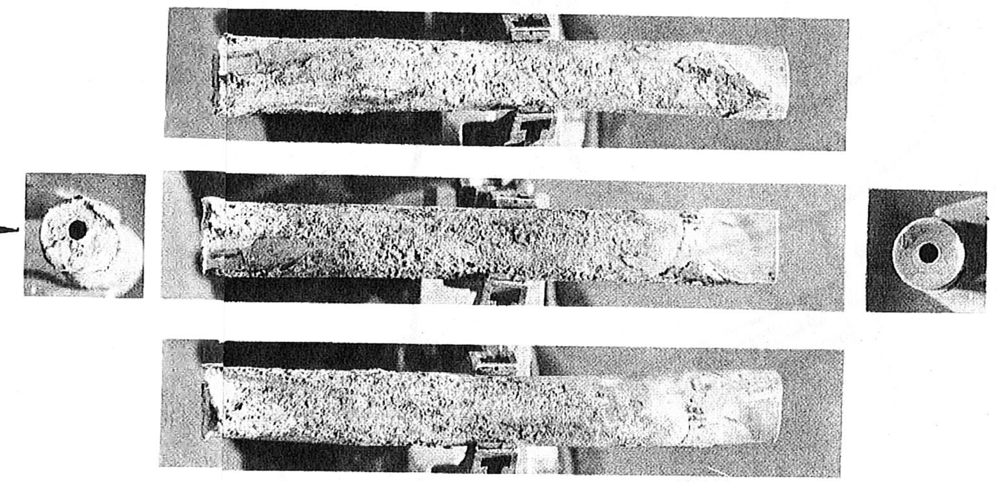

l. U - 1.8 Mo (583)

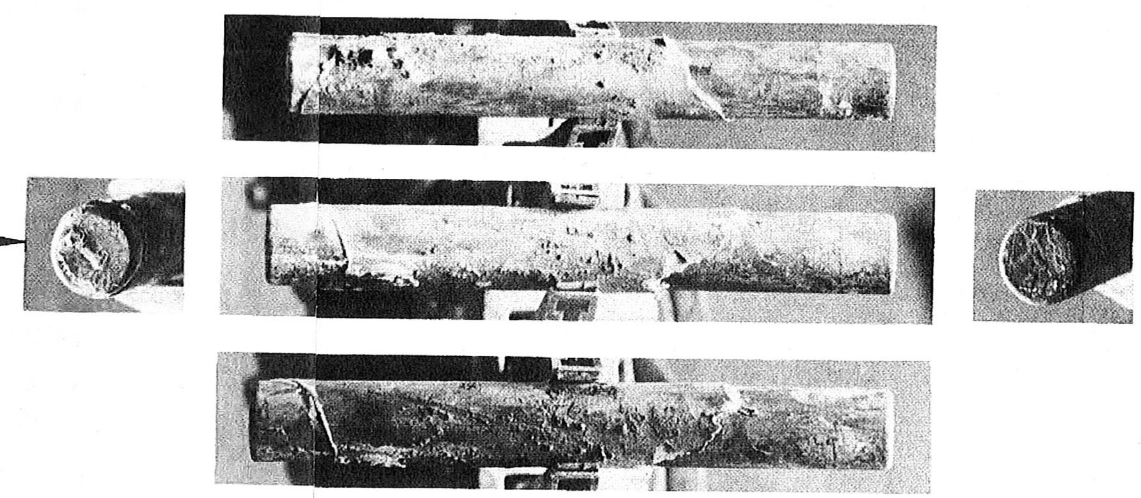

m. Th - 5.4 U (532)

6" LONG FUEL SLUG

0.750" ALL SLUG	0.750"	0.755"	0.755"	0.750"	0°
0.747"	0.751"	0.751"	0.751"	0.748"	90°

FUEL SLUG 335-4 FROM FUEL ROD 604 U - 3 Mo

0.749" ALL SLUG	0.744"	0.738"	0.735"	0.753"	0°
0.750"	0.750"	0.740"	0.718"	0.724"	90°

FUEL SLUG 73-B FROM FUEL ROD 572 U - 1.2 Mo

0.739" ALL SLUG	0.725"	0.700"	0.743"	0.750"	0°
0.734"	0.734"	0.720"	0.747"	0.768"	90°

FUEL SLUG 64N FROM FUEL ROD 583 U - 1.8 Mo

PART CLAD	ON CLAD	ON CLAD	PART CLAD	ALL SLUG	
0.786"	0.794"	0.803"	0.774"	0.747"	0°
ALL SLUG 0.746"	ALL CLAD 0.788"	ALL CLAD 0.796"	PART CLAD 0.769"	ALL SLUG 0.745"	90°

FUEL SLUG 0-3 FROM FUEL ROD 532 Th - 5.4 U.

n. Fuel Slug Measurements

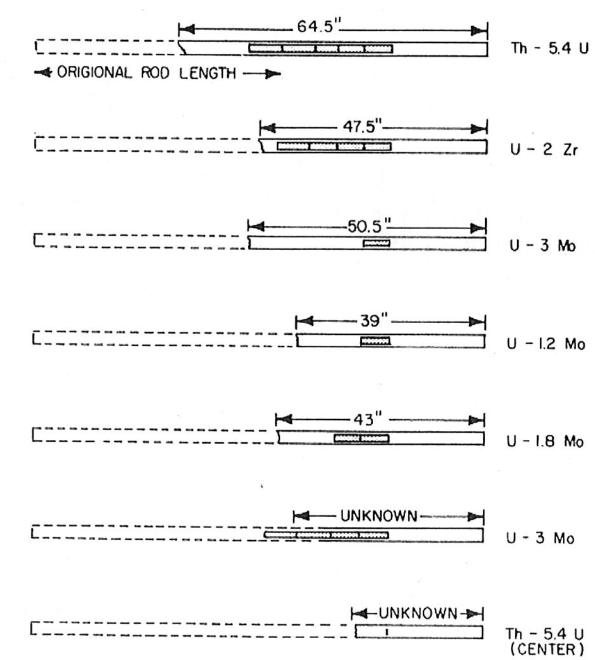

o. Length of Fuel Element Rods Recovered

ANALYSES OF MATERIALS FROM ELEMENT IN CHANNEL 55

Item Analyzed	Sample Condition	Analytical Method	Results	Remarks
1. Element 55 CDHC				
Cladding piece	As received As received	X-ray fluor. X-ray fluor.	90% U 10% U	Inside surface Outside surface
Cladding piece	Washed in conc. HNO_3	X-ray fluor. X-ray fluor.	1% U nil U	Inside surface Outside surface; also had a dull metallic luster
Cladding piece	Washed and soaked in conc. HNO_3 Washed and soaked in conc. HNO_3	Wet chem. Wet chem.	71.5% U 26.4% Fe 73% U 23.6% Fe	Total solution Total solution
Cladding piece	Washed and soaked in conc. HNO_3	Vacuum fusion	5030 ppm O_2 70 ppm H_2 120 ppm N_2	Duplicate samples for results
Cladding piece	Washed and soaked in conc. HNO_3	Conductometric and combustion	0.36% C	Total destructive test
Material taken from the element on inside of clad as received	In solution with conc. HNO_3	Wet chem.	70.6% U	Total sample run
2. Element 55 SRE				
Na residue from the top of fuel element	Dissolved in HCl	Wet chem.	17% Na 3% Fe 6% C	These values were calculated from weights given in report
Na residue from the top of fuel element	Dissolved in HNO_3	Combustion and X-ray fluor.	14.5% C	Includes CO_2 pickup
Wire wrap sample	Washed with conc. HNO_3	X-ray fluor.	nil U trace Mo	Solution analysis separate (metal only)
Wire wrap sample	Washed with conc. HNO_3	Wet chem.	82% U 8.8% Fe	Solution only
Wire wrap sample	HNO_3 cleaned metal sample	Combustion	0.11% C	

The first sample is from a piece of Fuel Element 55 that fell from fuel handling cask.

p. **Chemical Analysis of SU-2-5 (R-55)**

Figure 7. Evidence of Eutectic Melting

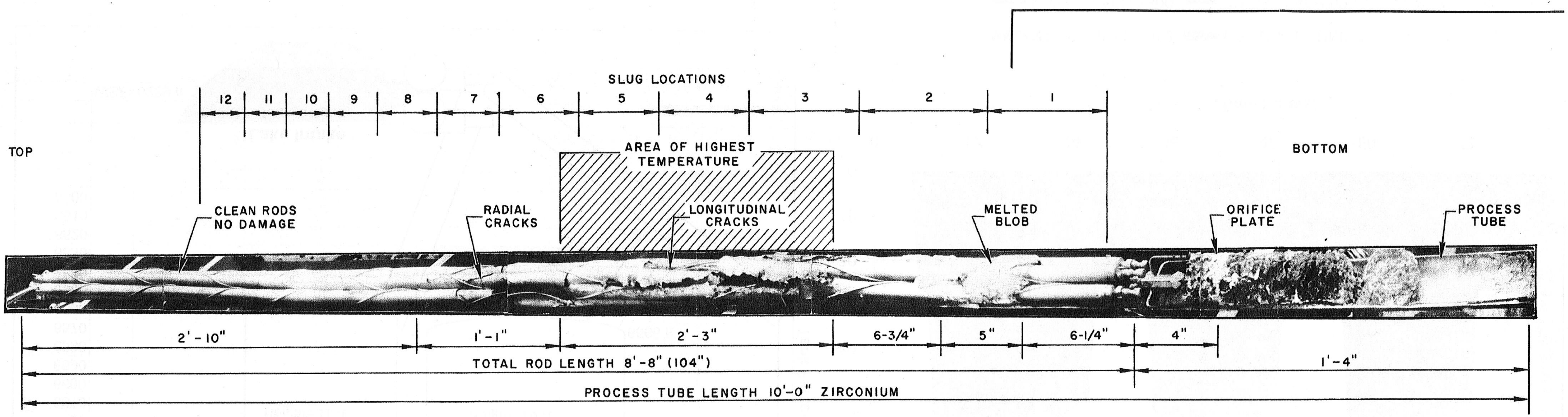

a. Composite of Fuel Element SU-1-15 (R-24)

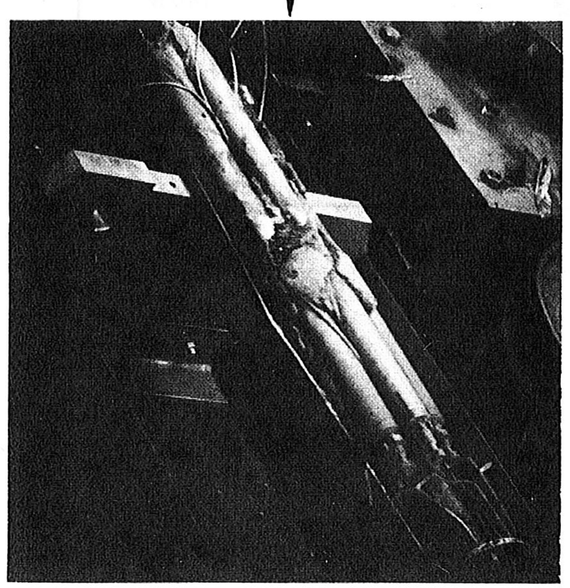

b.

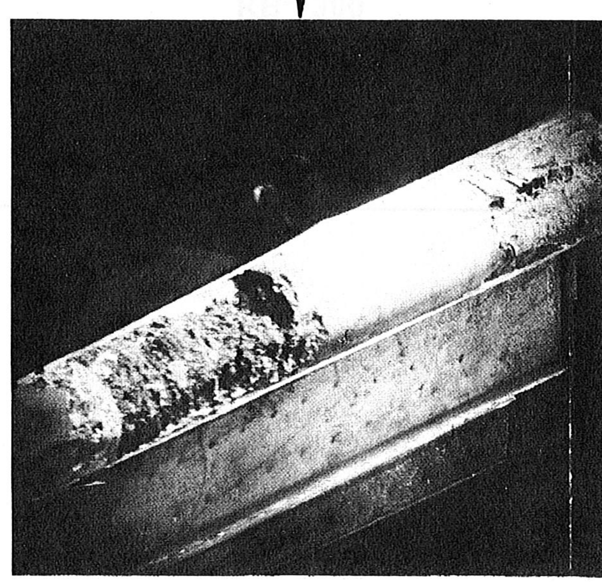

c.

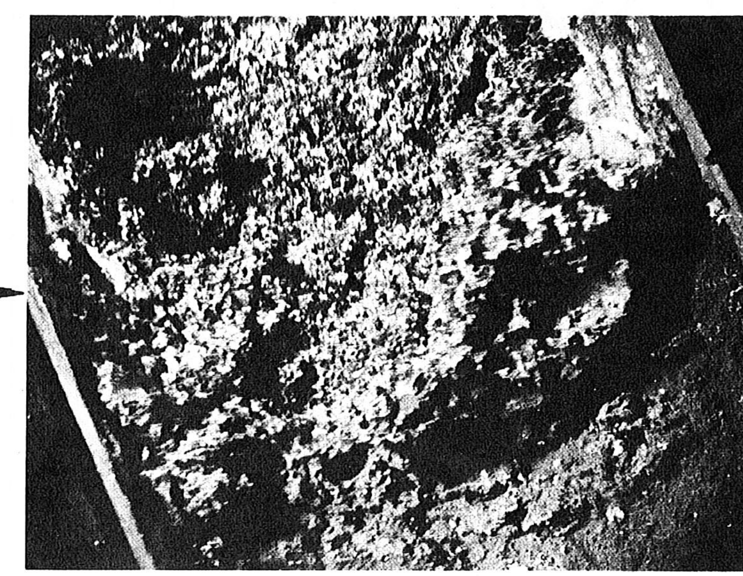

d.

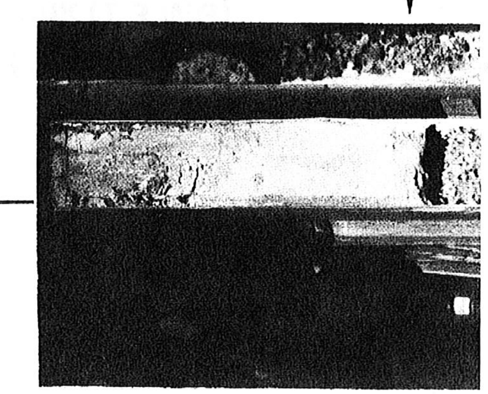

e.

FIGURE 8 LEFT

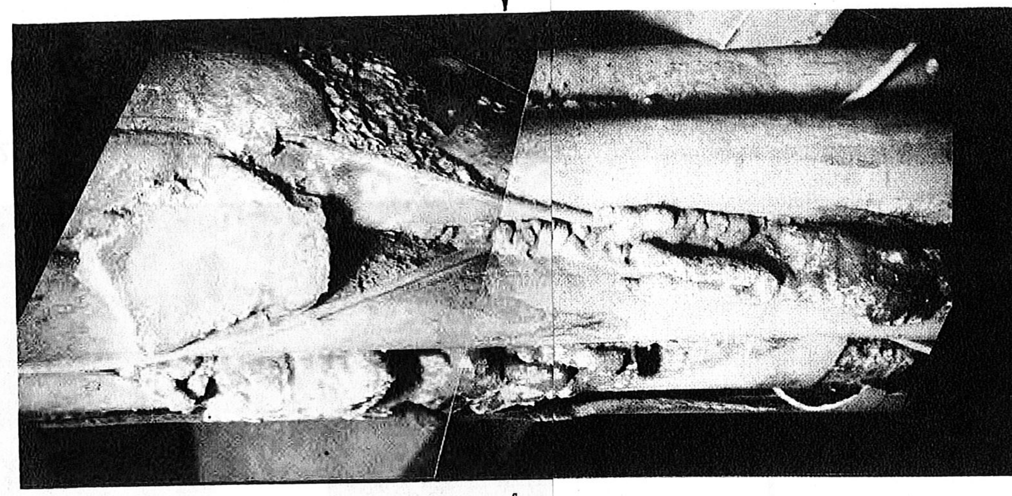

f.

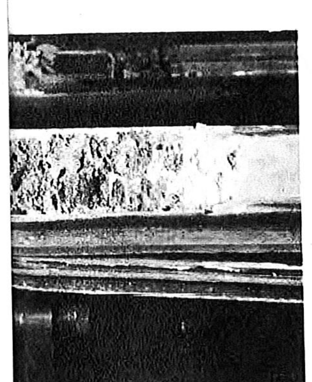

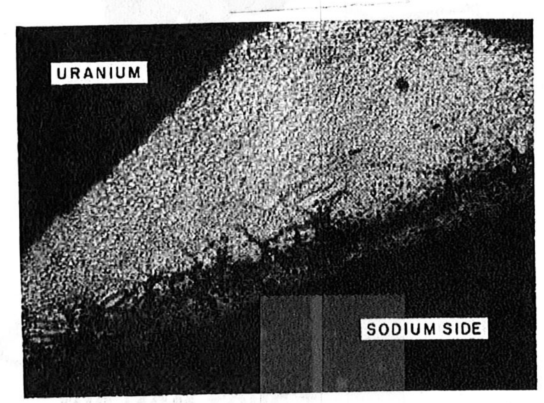

(1) 73X

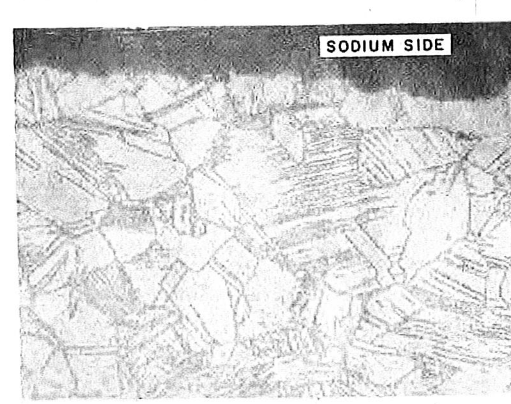

(2) 365X

(3) 110X

g. Photomicrographs of Cladding from SU-1-40 (R-25), Adjacent to Melted Area

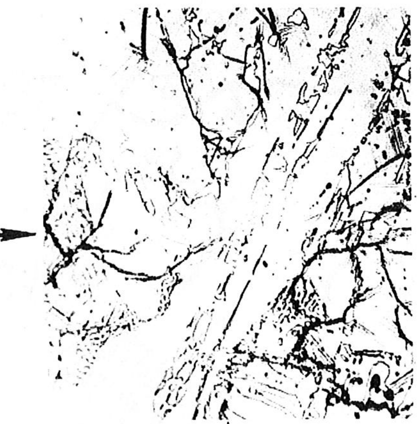

Etched 250X
(1) Irradiated

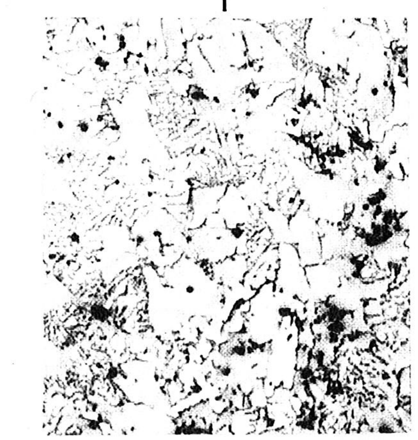

Etched 250X
(2) Unirradiated

h. Photomicrograph of Melted Material

Figure 8. Evidence of Eutectic Melting and Plugging of the Fuel Channel

NAA-SR-4515

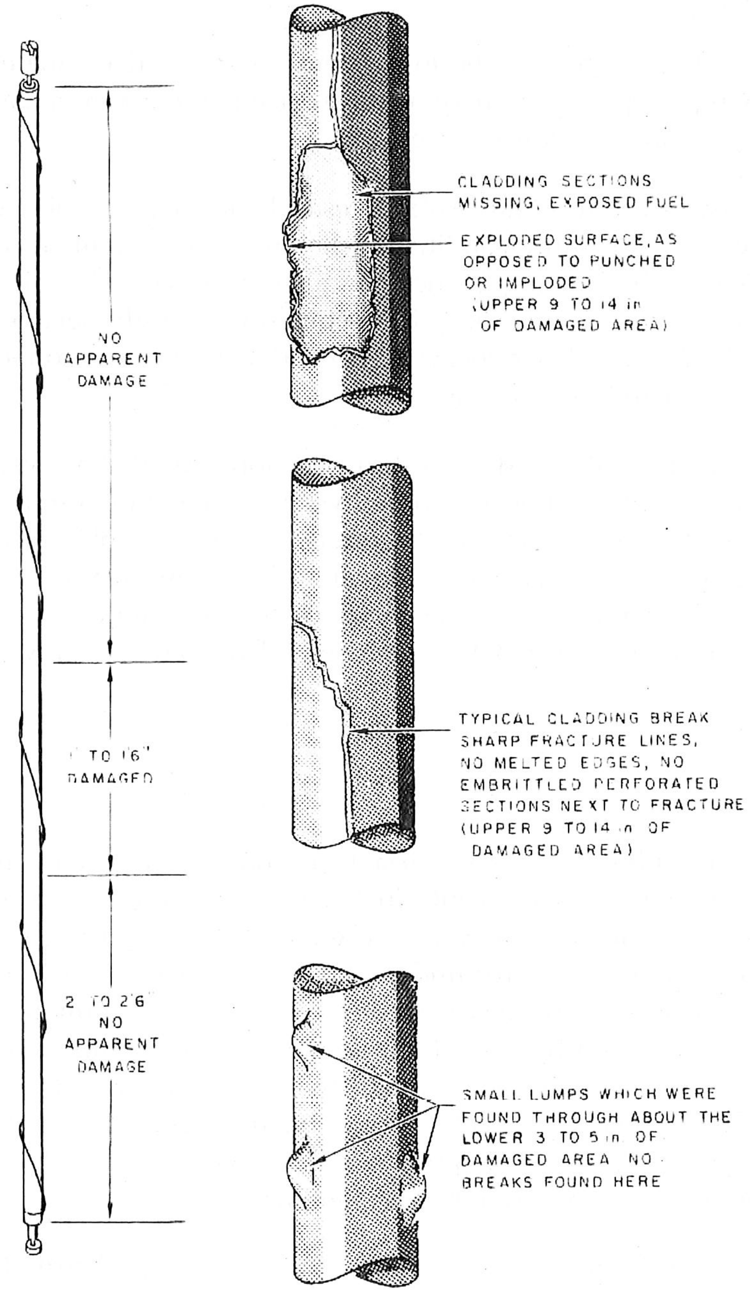

a. Location and Description of Typical Breaks

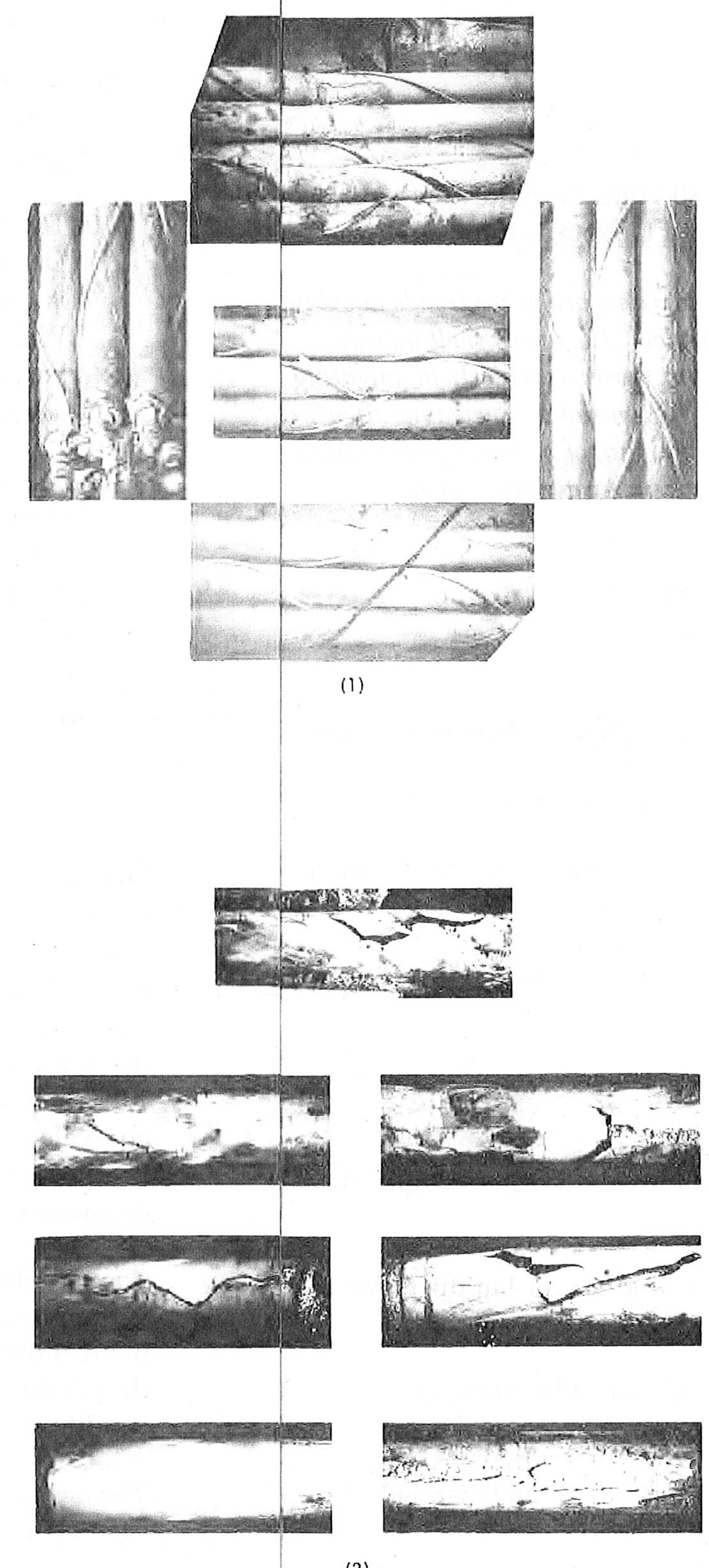

b. Fuel Element SU-1-4(R-25)

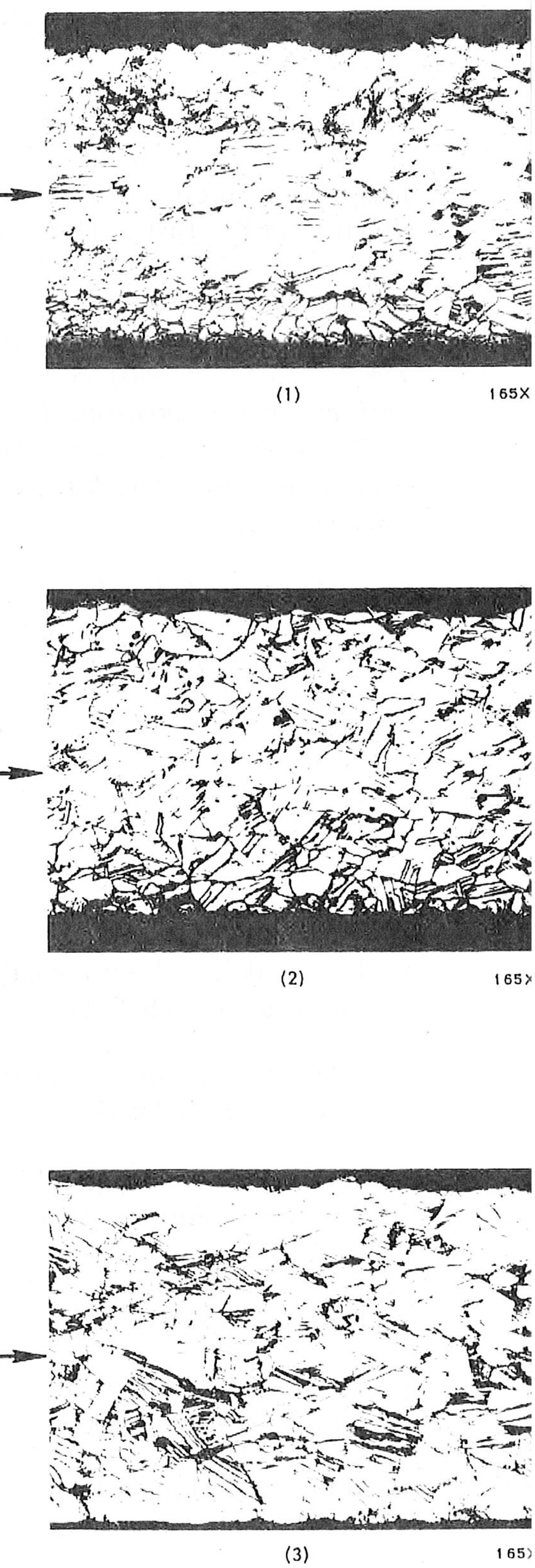

c. Photomicrographs of Cladding

Figure 9 - left hand side

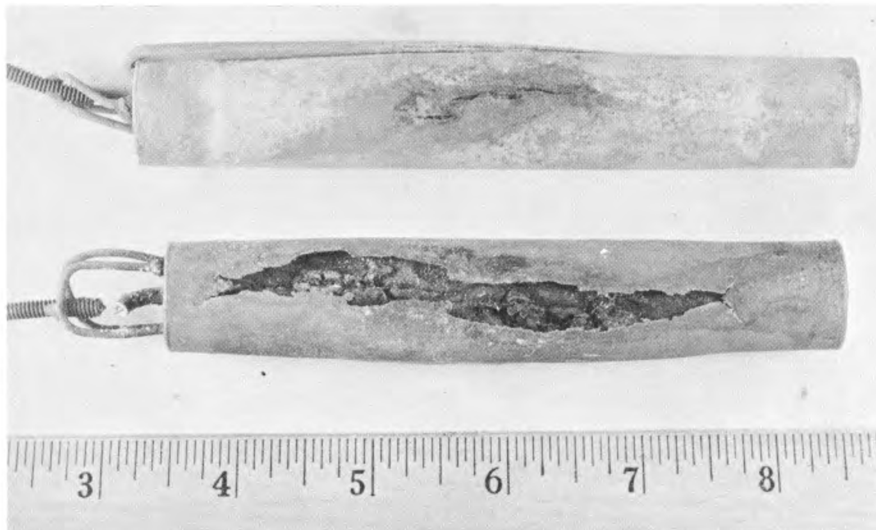

d. Thermal Cycled Test Capsules

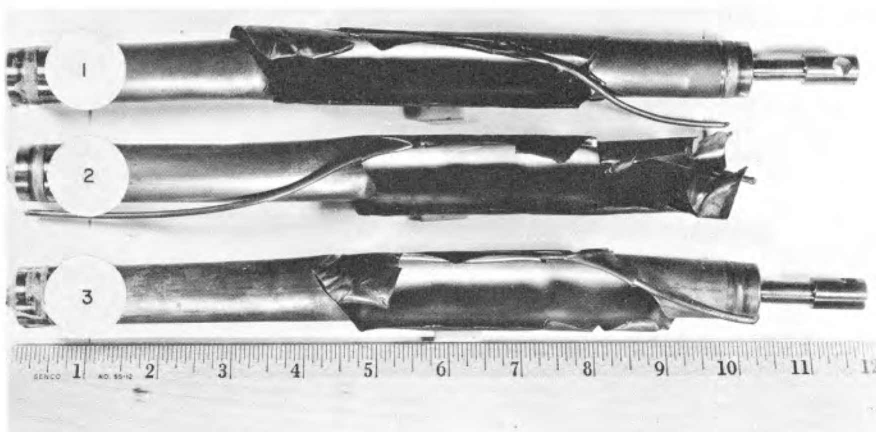

e. Pressure Tested Wire Wrapped Test Capsules

Figure 9. Results Supporting Thermal Cycling Thesis

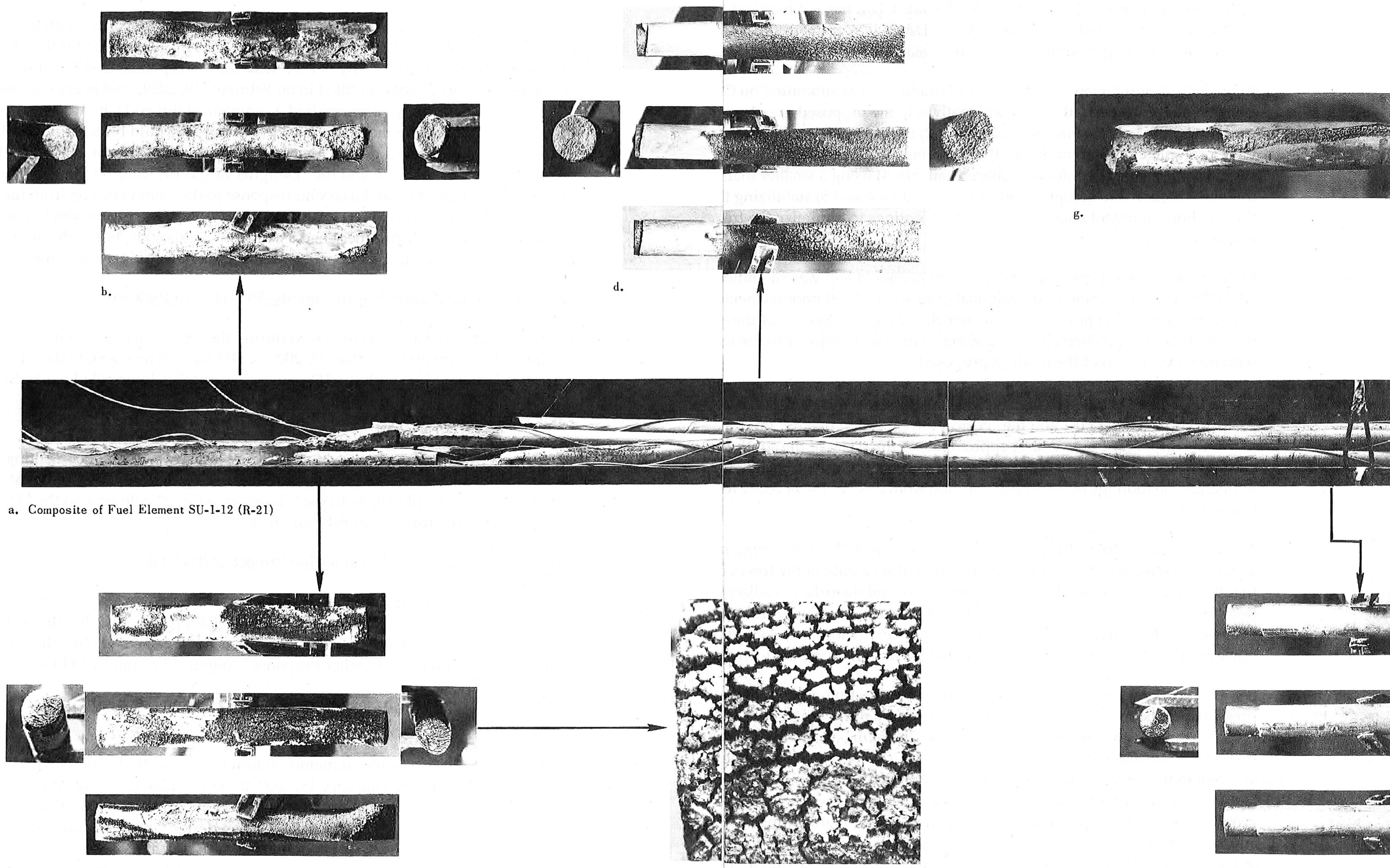

b.

d.

g.

a. Composite of Fuel Element SU-1-12 (R-21)

c.

f. 3X

e.

FIGURE 10 LEFT

Distance From Top of Rod (in.)	Diameter (in.)		Distance From Top of Rod (in.)	Diameter (in.)		Distance From Top of Rod (in.)	Diameter (in.)	
	Initial Reading	Rod Rotated 90°		Initial Reading	Rod Rotated 90°		Initial Reading	Rod Rotated 90°
Rod No. 1			Rod No. 3			Rod No. 5		
24	0.791	0.791	3	0.792	0.790	1	0.791	0.790
59	0.786		23	0.790	0.790	16	0.794	0.794
60	0.785	0.790	39	0.790	0.785	32	0.791	0.788
61	0.786		40	0.785	0.782	48	0.794	0.790
62	0.785		41	0.788	0.786	64	0.790	0.790
63	0.783		42	0.791	0.790	80	0.790	0.790
90	0.785	0.791	60	0.791	0.790	91	0.792	0.789
			90	0.790	0.792			
Rod No. 2			Rod No. 4			Rod No. 6		
23	0.790		3	0.791	0.791	1	0.790	0.790
24	0.792	0.789	23	0.792	0.790	16	0.792	
60	0.790	0.791	40	0.791	0.790	24	0.791	0.790
90	0.792	0.790	60	0.790	0.791	40	0.794	0.786
			87	0.791	0.792	56	0.790	0.790
						72	0.788	0.790
						91	0.791	0.790

l. Clad Rod Measurements

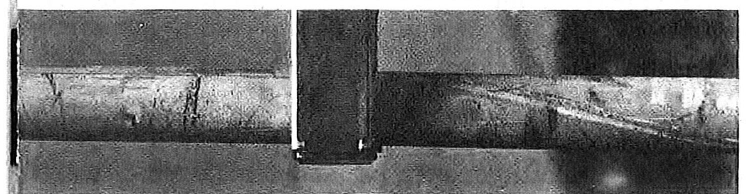

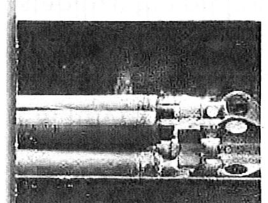

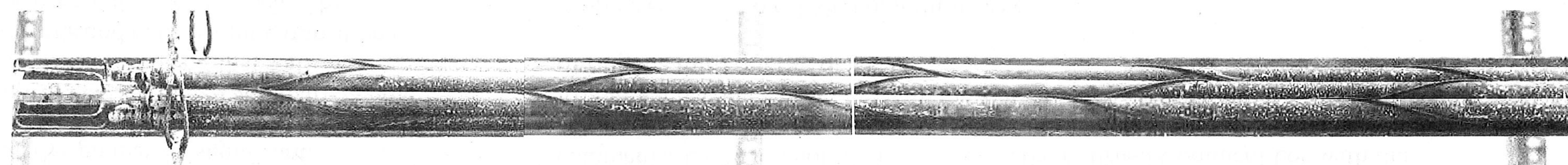

h. Composite of Fuel Element SU-1-20 (R-45)

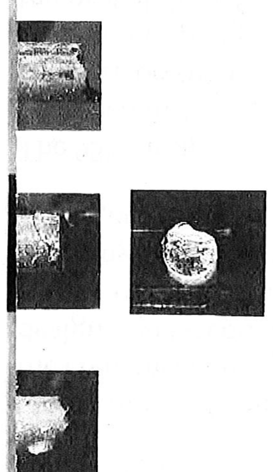

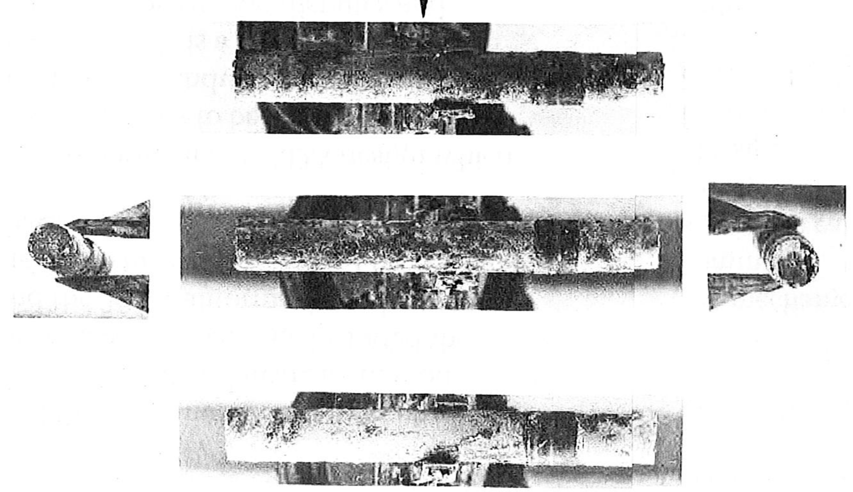

i.

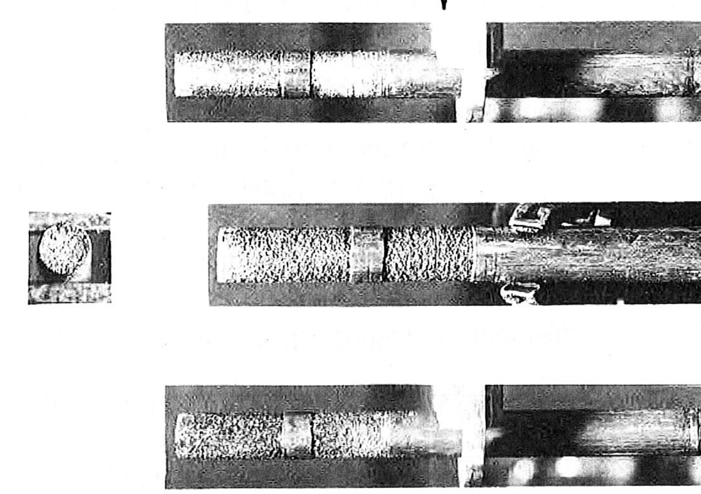

j.

FIGURE 10 CENTER

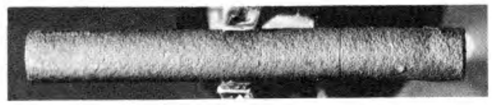

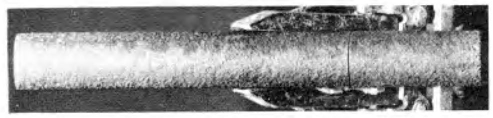

k.

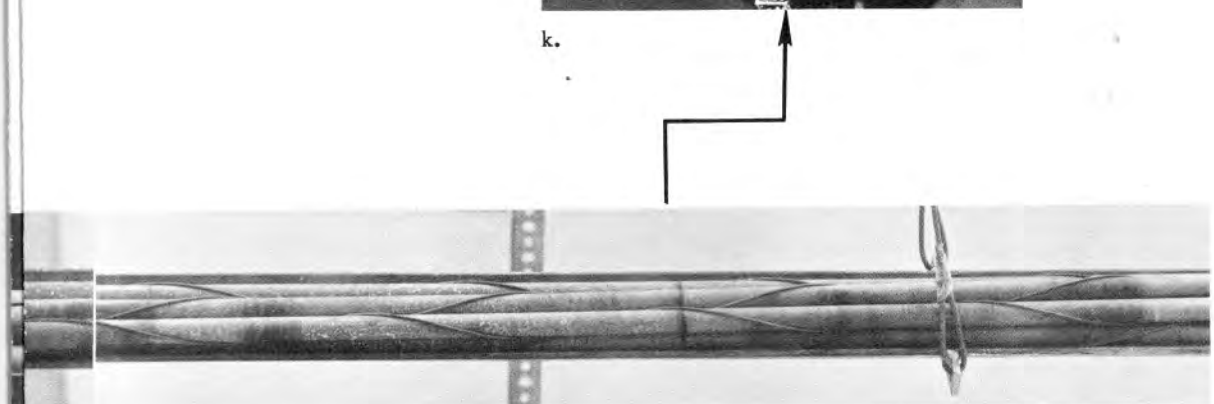

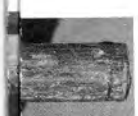

Diameter of Slug (in.)		Diameter of Slug (in.)	
Initial Reading	Slug Rotated 90° on Axis	Initial Reading	Slug Rotated 90° on Axis
0.751	0.749	0.753	0.745
0.750	0.751	0.751	0.737
0.747	0.748	0.741	0.745
0.750	0.751	0.748	0.740
0.756	0.751	0.743	0.752

Diameter of Slug (in.)		Diameter of Slug (in.)	
Initial Reading	Slug Rotated 90° on Axis	Initial Reading	Slug Rotated 90° on Axis
0.749	0.751	0.752	0.750
0.749	0.751	0.750	0.750
0.749	0.750	0.750	0.750
0.751	0.750	0.789*	0.784*
		0.790*	0.790*

*Reading taken on cladding.

m. Unclad Slug Measurements

Figure 10. Results Supporting Thermal Cycling Thesis and Plugging Phenomenon

a. Central Fuel Temperatures of Fuel Element SU-2-5 (R-55)

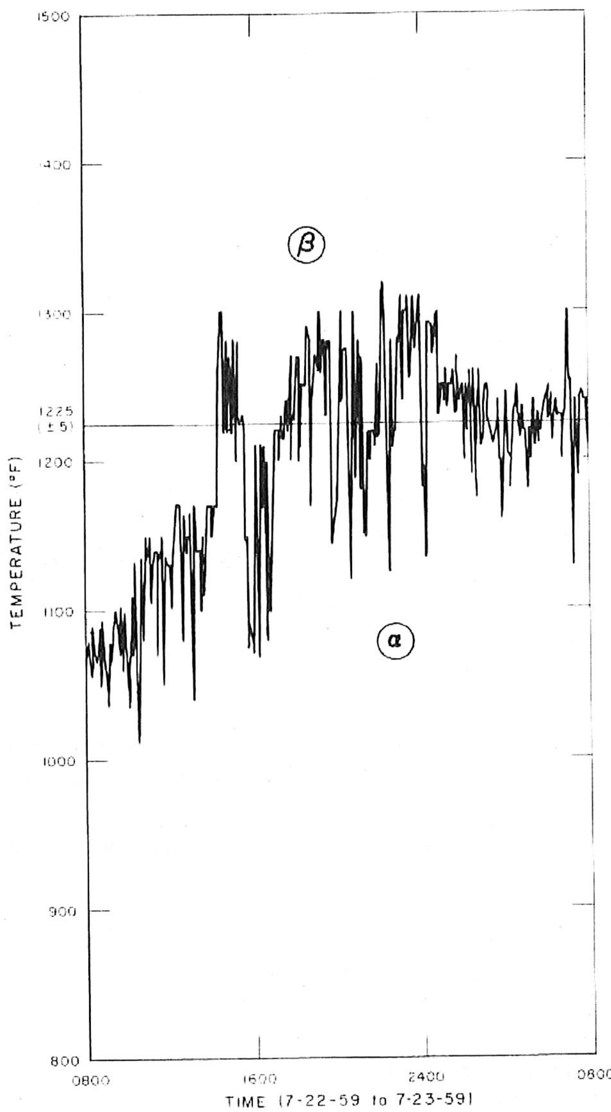

(1) 15 in. in Fuel

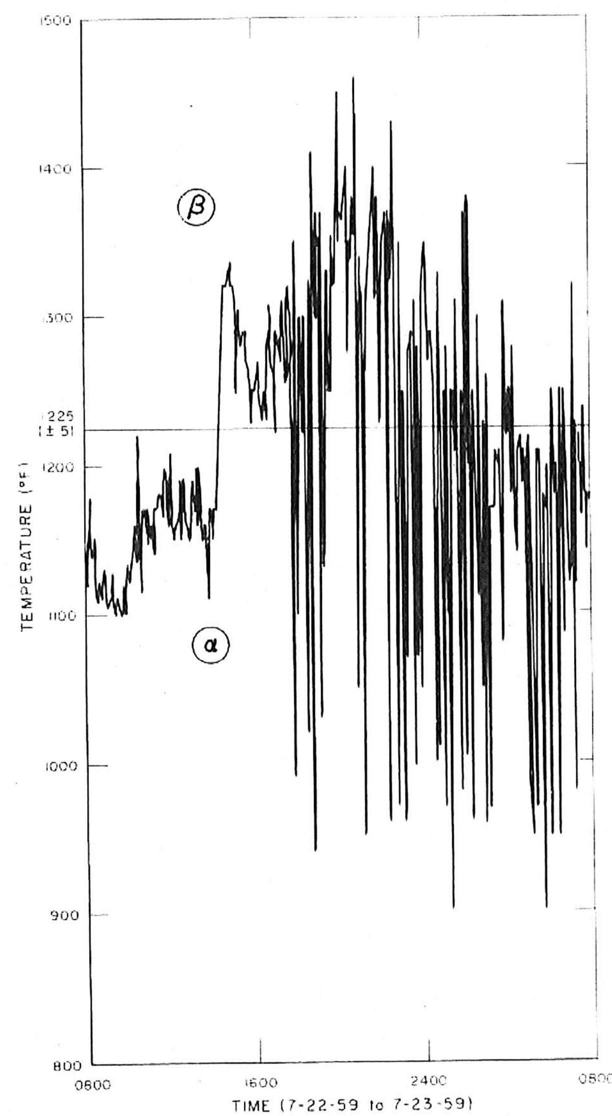

(2) 25 in. in Fuel

b. Exit Sodium Temperatures

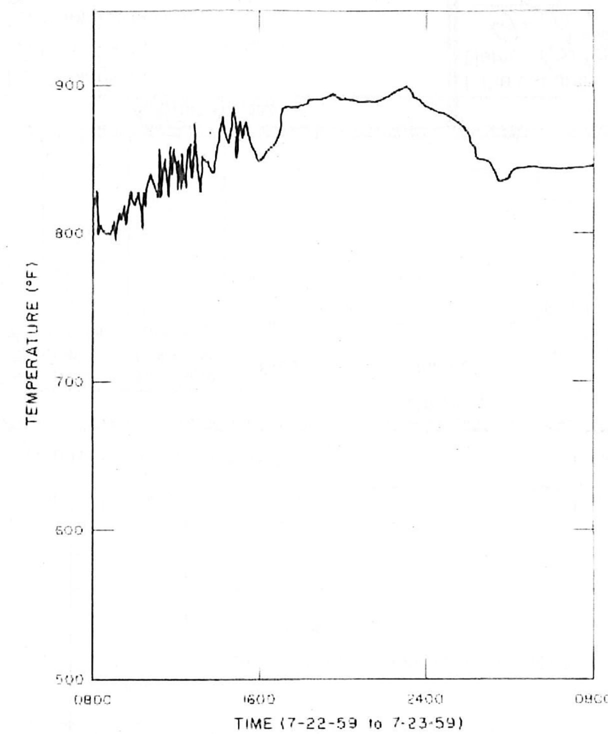

(1) Fuel Element SU-1-40 (R-25)
(Damaged)

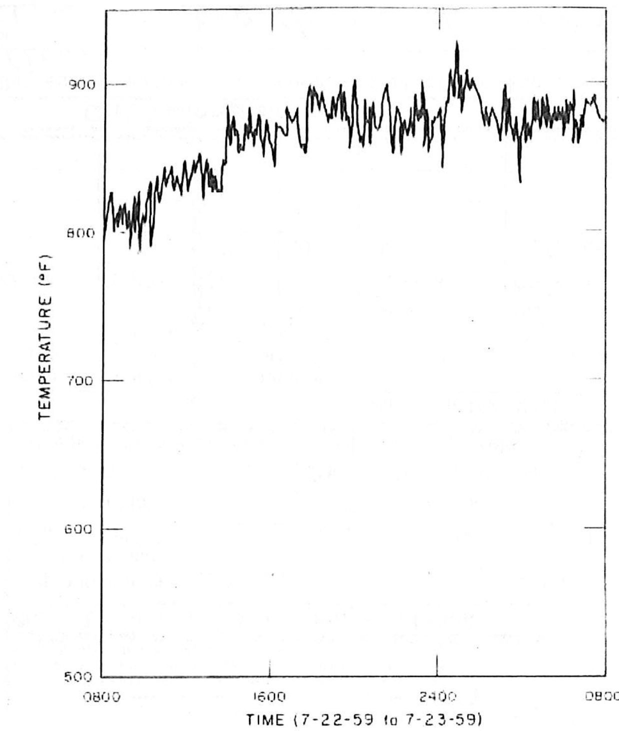

(2) Fuel Element SU-1-15 (R-24)
(Damaged)

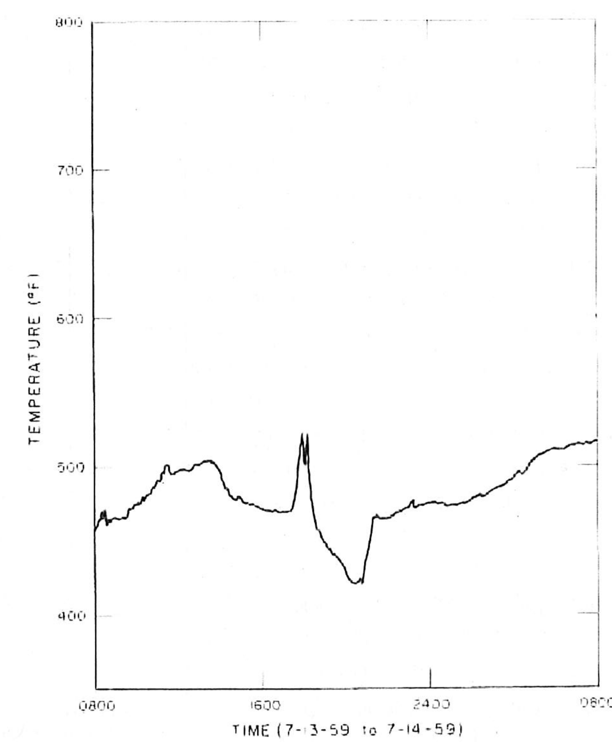

(3) Fuel Element SU-1-26 (R-67)
(Undamaged)

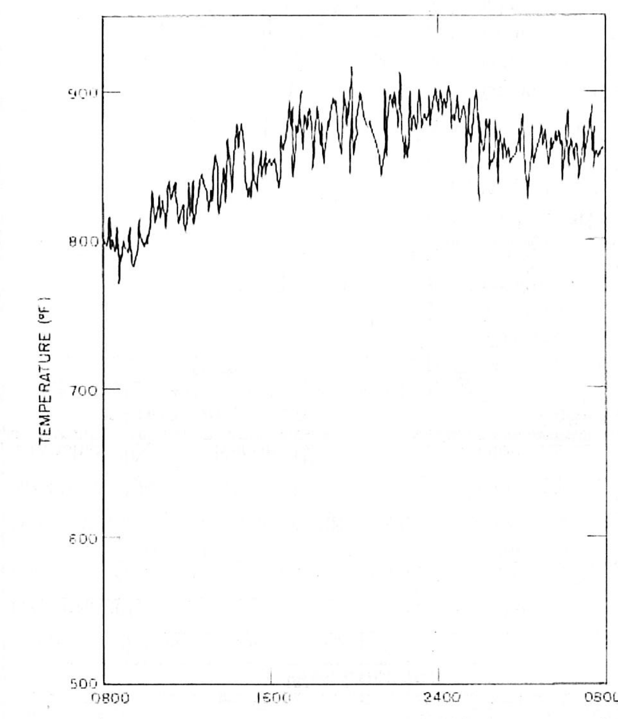

(4) Fuel Element SU-2-3 (R-43)
(Damaged)

Figure 11. Temperature Information Supporting Thermal Cycling Thesis

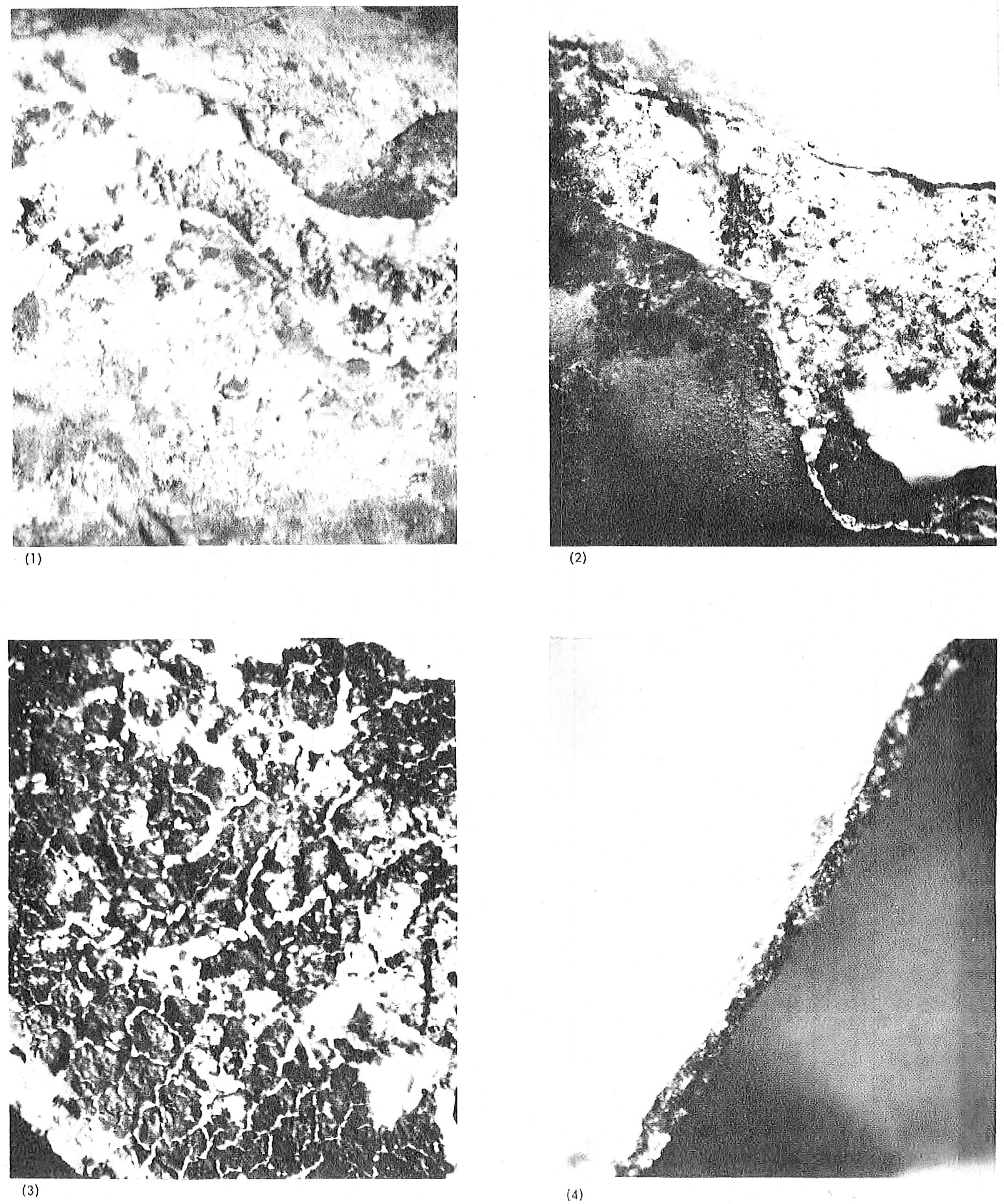

a. Fuel and Cladding from SU-1-9 (R-12)

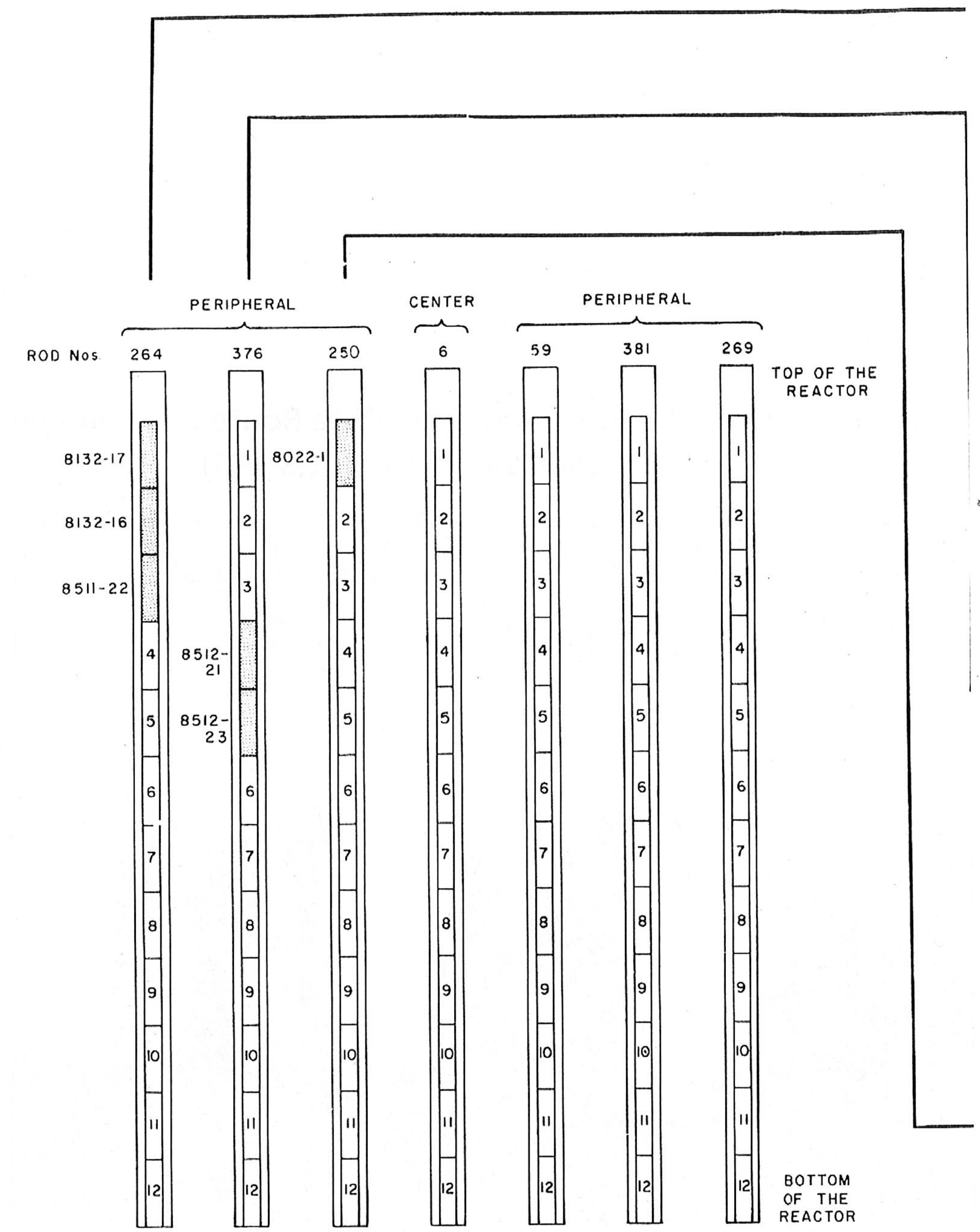

b. Location of Fuel Slugs Recovered from Element SU-1-9 (R-12)

FIGURE 12 LEFT

Location of Measurement*	Diameter (in.)	Location of Measurement*	Diameter (in.)
Rod No. 264			
Slug No. 8132-17			
SLUG No. 8132-17			
1 a	0.769	1 b	0.792
1.5 a	0.770	1.5 b	0.793
2 a	0.771	2 b	0.789
2.5 a	0.773	2.5 b	0.792
3 a	0.769	3 b	0.791
3.5 a	0.767	3.5 b	0.790
4 a	0.768	4 b	0.789
4.5 a	0.790	4.5 b	0.790
5 a	0.782	5 b	0.772
5.5 a	0.778	5.5 b	0.793
Slugs No. 8132-16 and 8511-22			
SLUG No 8132-16		SLUG No 8511-22	
1 a	0.770	1 b	0.765
2 a	0.775	3 b	0.767
3 a	0.772	4 b	0.767
4 a	0.774	5 b	0.778
5 a	0.779	6 b	0.761
6 a	0.829	7 b	0.827
7 a	0.855	8 b	0.848
8 a	0.907	9 b	0.836
9 a	0.933	10 b	0.871
10 a	0.923		
11 a	0.952		
Rod No. 376			
Slugs No. 8512-21 and 8512-23†			
SLUG No 8512-12		SLUG No 8512 23	
2 a	0.878	10 a	0.873§
2 b	0.891	10 b	0.870
2 c	0.857	10 c	0.861
2 d	0.868§	10 d	0.861
2 e	0.886§	10 e	0.870§
4 a	0.873§	12 a	0.883§
4 b	0.852	12 b	0.887
4 c	0.863	12 c	0.878
4 d	0.847	12 d	0.886
4 e	0.846§	12 e	0.830§
6 a	0.868§		
6 b	0.860		
6 c	0.847		
6 d	0.833		
6 e	0.854§		
Rod No. 250			
Slug No. 8022-1			
SLUG No 8022-1			
0 a	0.784	6 a	0.801
0 b	0.781	6 b	0.805
0 c	0.781	6 c	0.808
0 d	0.788	6 d	0.818
0 e	0.784	6 e	0.823
3 a	0.787		
3 b	0.822		
3 c	0.824		
3 d	0.817		
3 e	0.814		

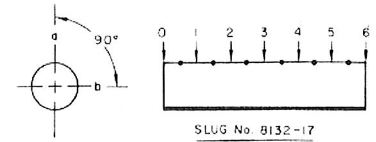

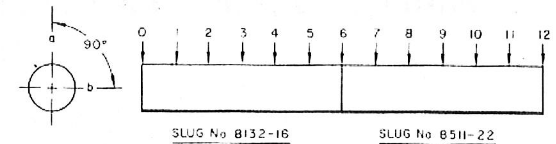

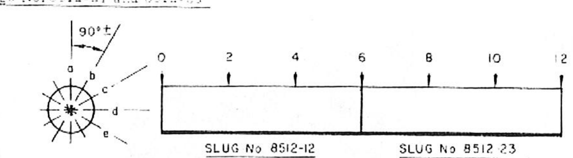

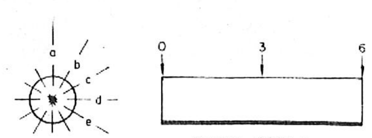

*Numbers indicate inches from numbered end of slug, letters indicate rotation of slug (shown in figures).
†Dimensions are of fuel slugs plus cladding unless noted otherwise (nominal cladding 0.790 in.OD).
§Near split in cladding.

c. Dimensions of Recovered Fuel Slugs

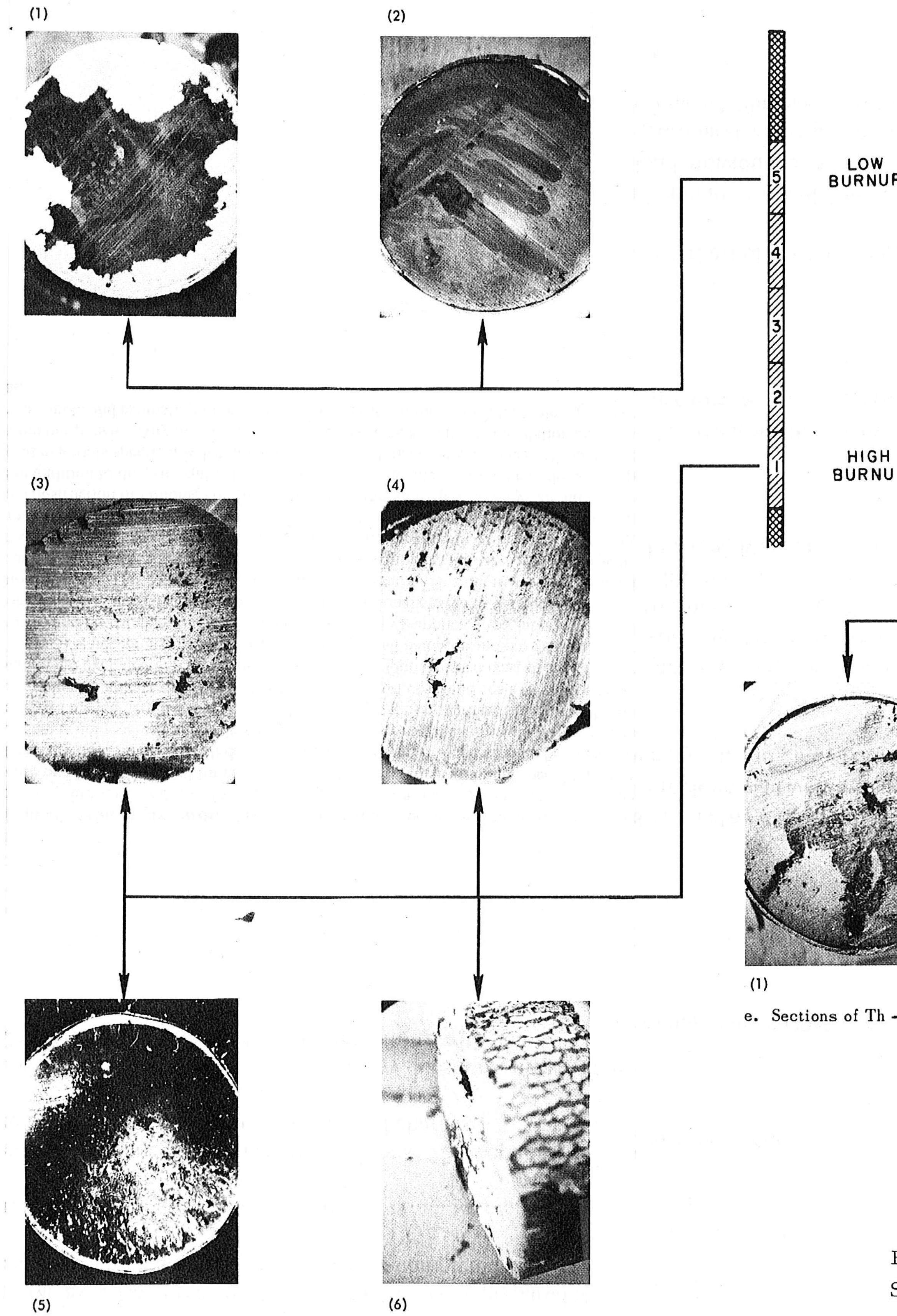

d. Sections of Unalloyed Uranium from Element SU-1-12 (R-21)

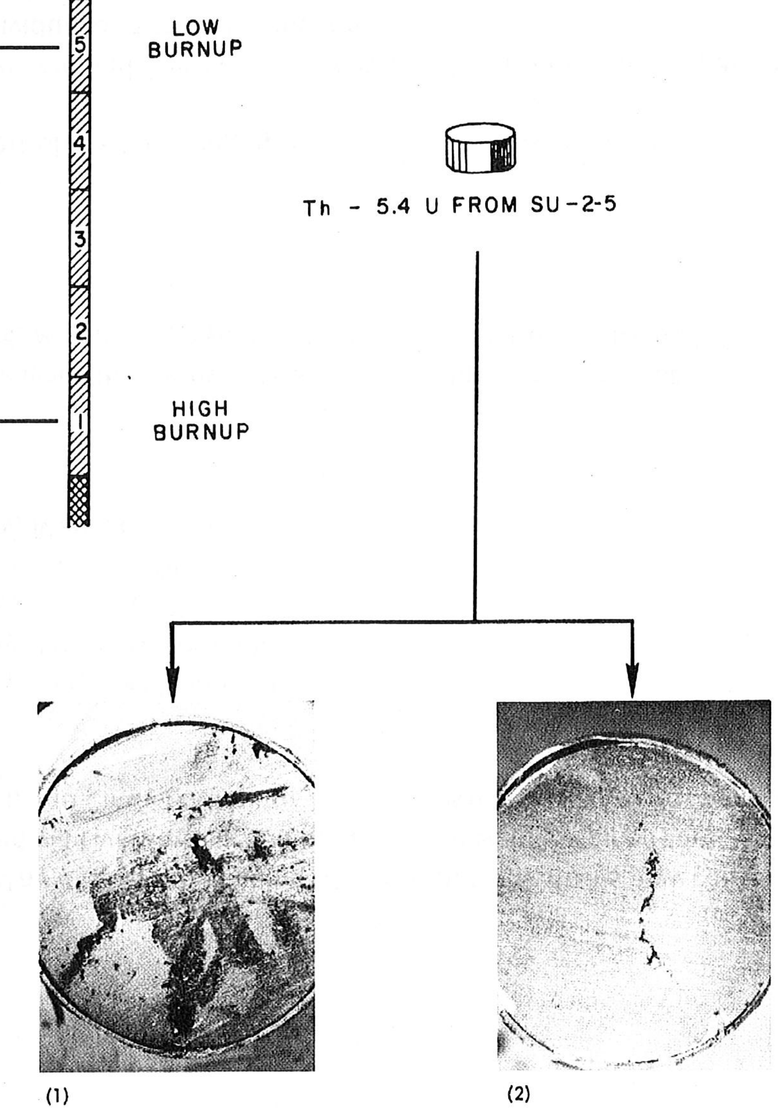

e. Sections of Th - 5.4 U from Element SU-2-5 (R-55)

Figure 12. Supplementary Results Supporting Thermal Cycling Thesis

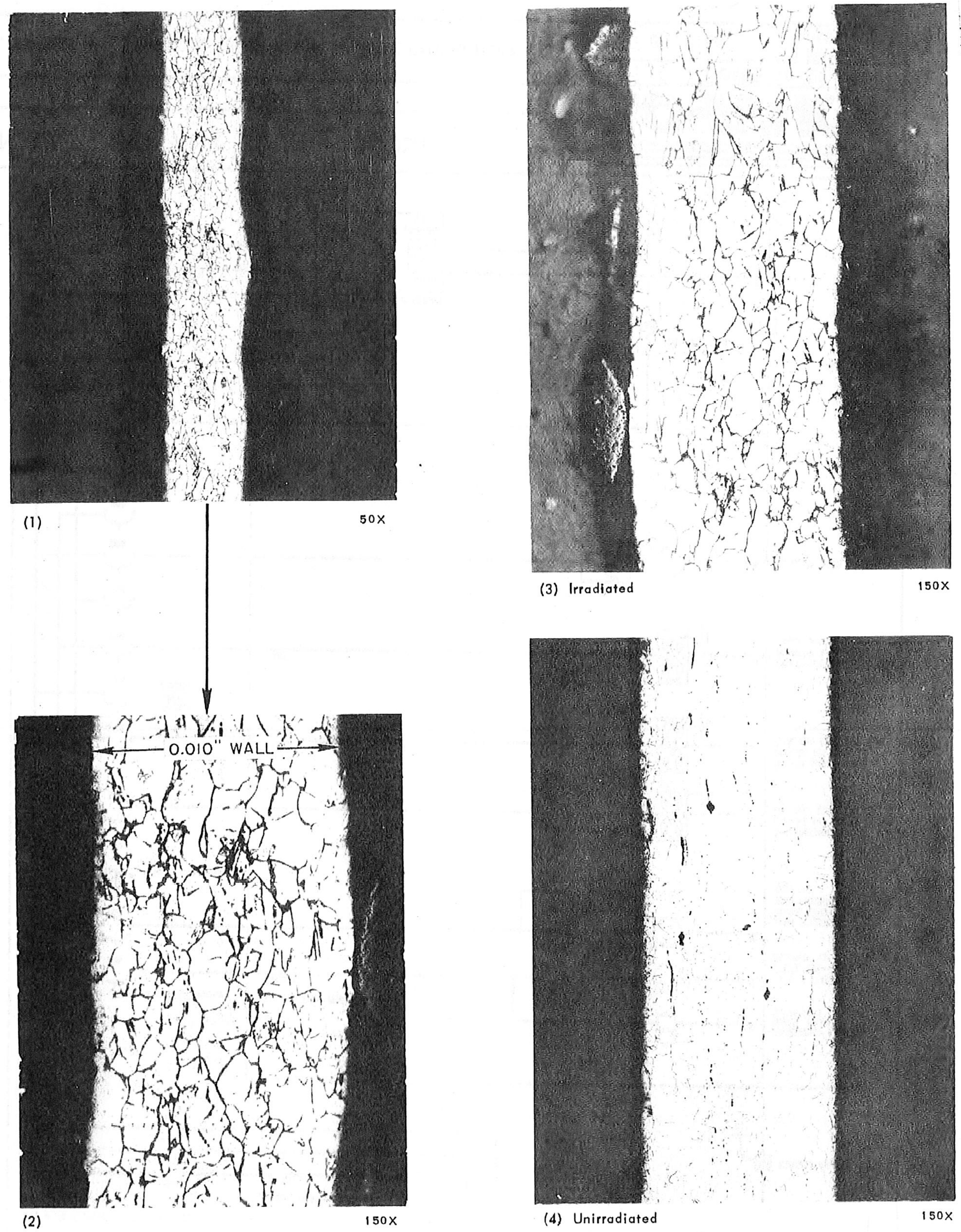

a. Cladding from Fuel Element SU-1-3 (R-56) (Type 304 Stainless Steel)

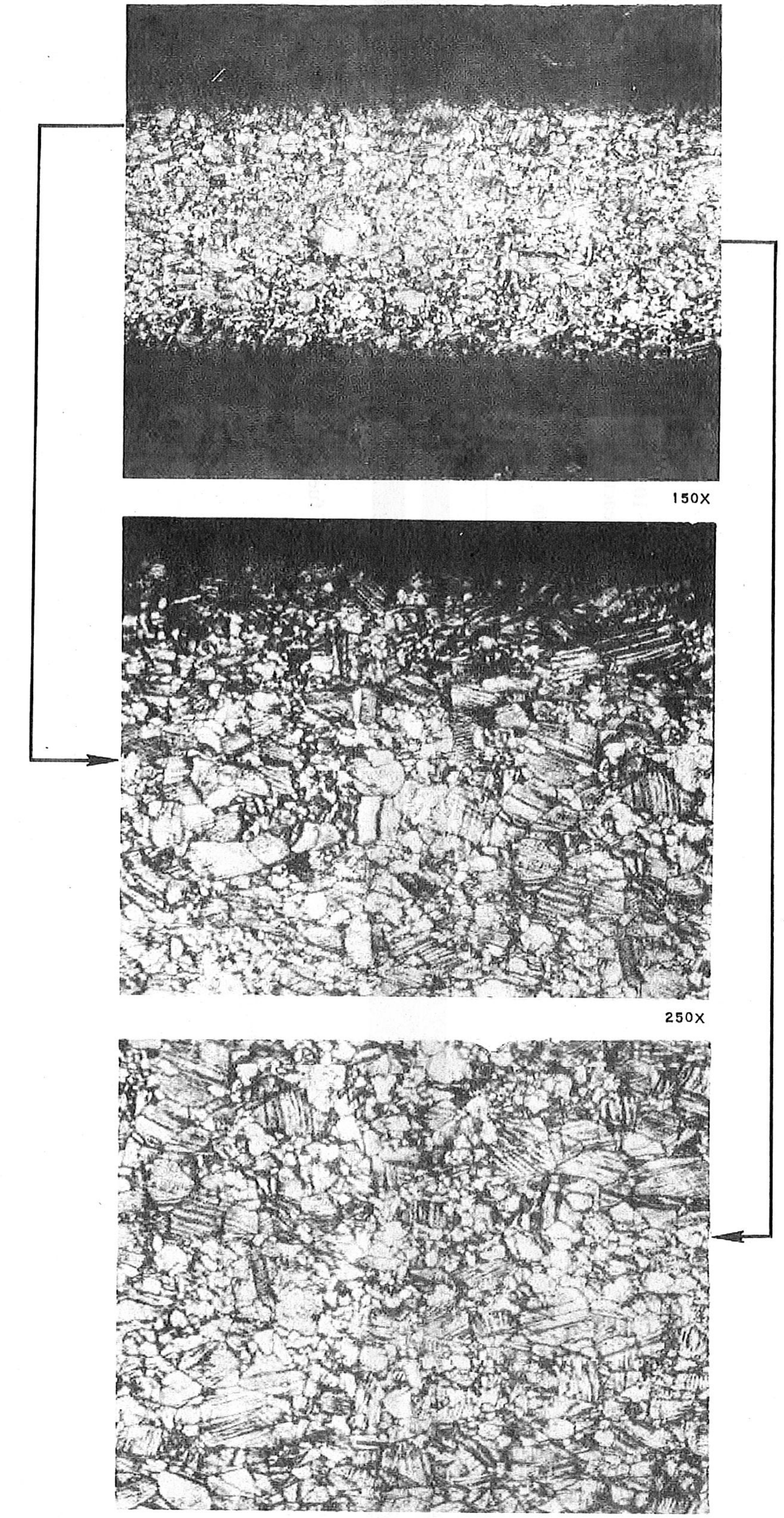

b. Cotter Pin from Fuel Element SU-1-3 (R-56)

FIGURE 13 LEFT

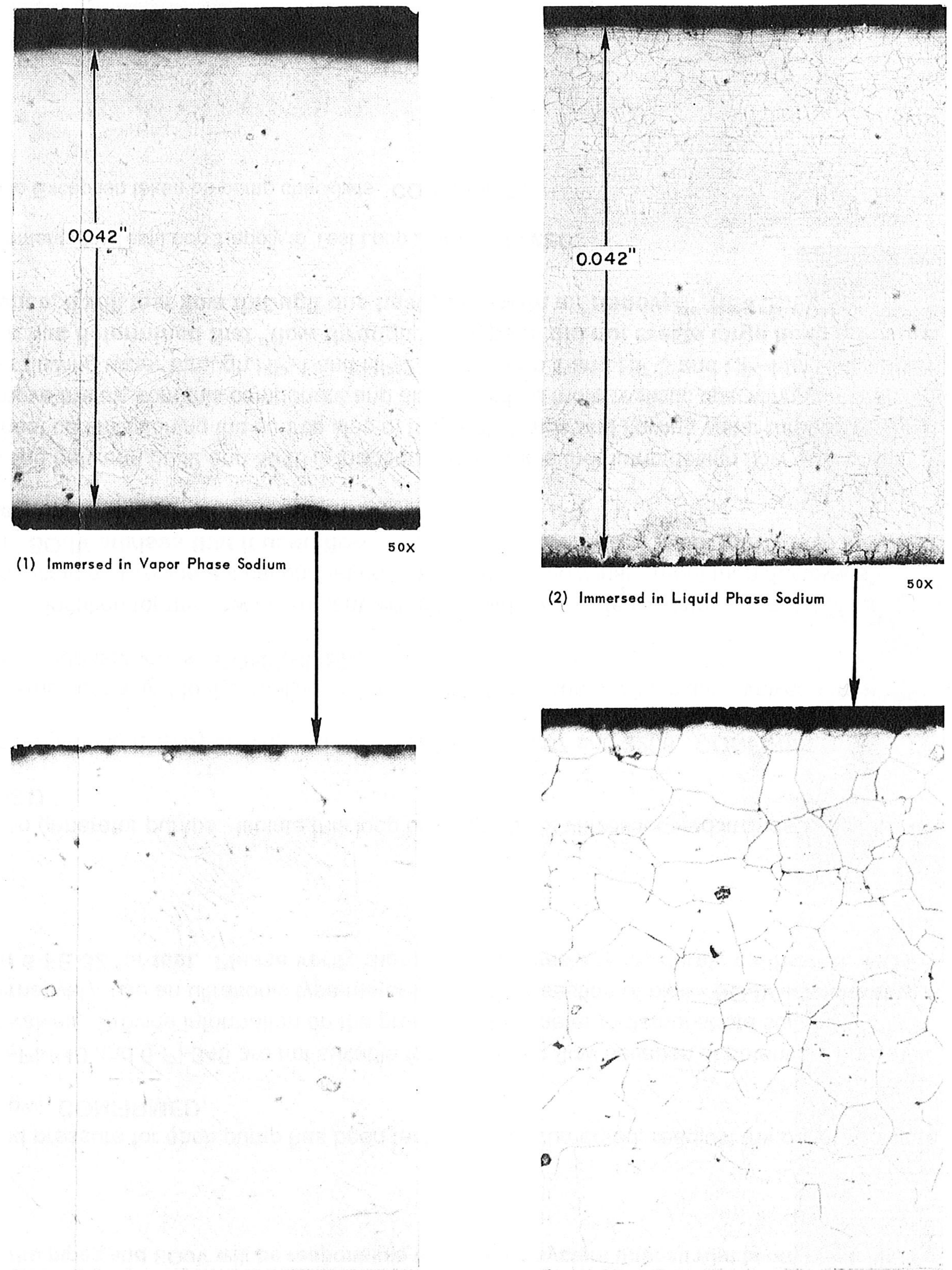

(1) Immersed in Vapor Phase Sodium

(2) Immersed in Liquid Phase Sodium

c. Upper Hardware (Hanger Rod Hold-down Tube) from Element SU-1-3 (R-56)

	Diagonal (long) (filar)	Diagonal (long) (mm)	Knoop Number	R_c*	R_b*
Edge	152	0.070	290	27	
	141	0.065	337	33	
	160	0.074	260	22	
	171	0.079	228	< 20	95.5
	171	0.079	228		95.5
	171	0.079	228		95.5
	172	0.0795	225		95
	187	0.086	192		88
Etched	175	0.081	217		93
	177	0.082	212		92
	175	0.081	217	< 20	93
	163	0.075	253	20.5	
	163	0.075	253	20.5	
	154	0.071	282	26	
Edge	150	0.069	299	28	
	138	0.064	347	34.5	

Spacing of indentations 0.1 mm, except at edges.

*Conversion of Knoop to R_c and R_b is from table, and therefore is only relative.

Knoop indentor 100 g load
10.25 objective
1 filar unit = 0.000462 mm

d. Results of Microhardness Testing

Figure 13. Results Indicating Absence of Structural Damage from Nitriding or Carburization

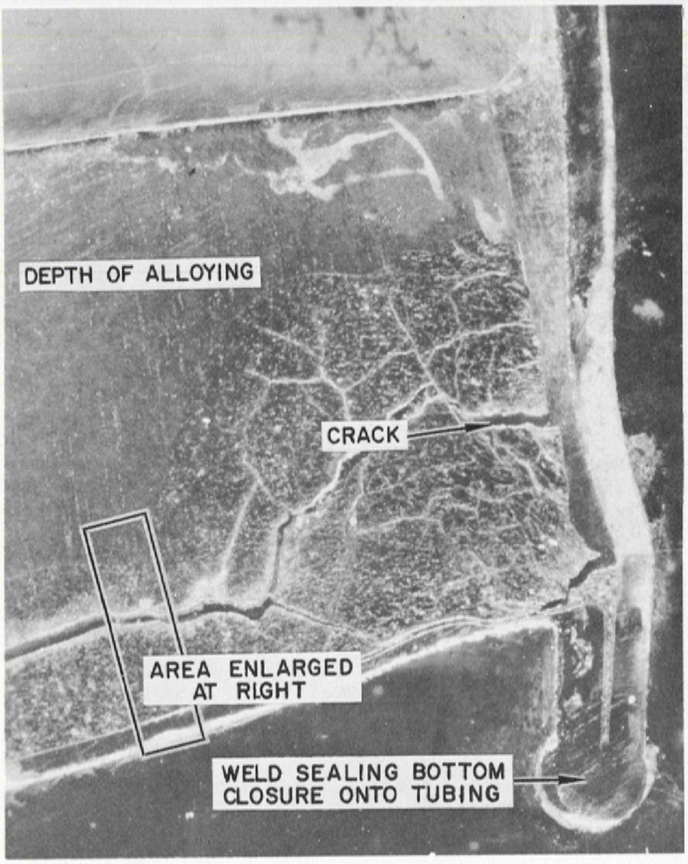

a. Typical Cross Section

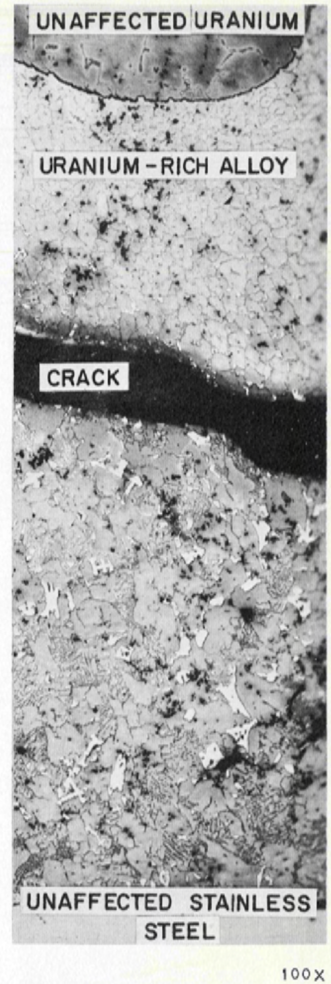

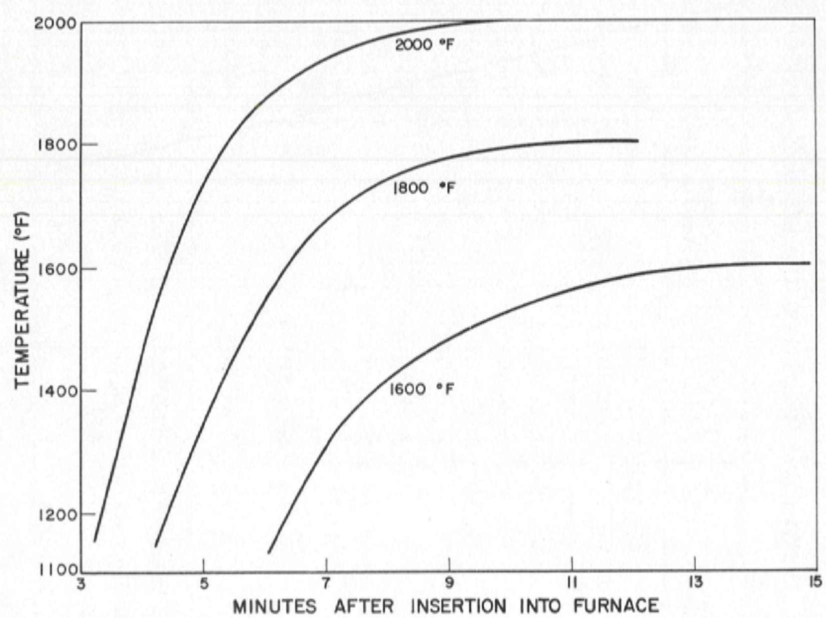

b. Time for Reaction

Figure 14. Corroborative Evidence on Reaction of Uranium Alloys with Stainless Steel

TABLE II

RECAP OF HOT CELL EXAMINATIONS FOR SRE FUEL ELEMENT DAMAGE EPISODE

Test No.	Date of Test	Experiment Number	Burnup (Mwd/MTU)	Item Observed	Tests Applied To Samples					Condition Of Element
					Visual	Met	Chem	Dim	Other	
1	Aug 59	R-55 SU2-5	733	Piece of cladding	yes	yes	yes	no	Cladding bend tests	Damaged
2	Sept 59	R-12 SU1-9	747	Sections of rod	yes	yes*	yes*	yes	Cladding bend tests	Damaged
3	Nov 59	R-55 SU2-5	733	Remainder of element	yes	yes	yes*	yes	Cladding bend tests	Damaged
4	Nov 59	R-21 SU1-12	852	Remainder of element	yes	yes	yes*	yes	Cladding bend tests	Damaged
5	Nov 59	R-45 SU1-20	876	Whole element	yes	yes	no	yes	Cladding bend tests	Good
6	Feb 60	R-67 SU1-26	505	Whole element	yes	yes	no	yes	Cladding bend tests	Good
		R-73 SU1-34	735	Whole element	yes	yes	no	yes	Cladding bend tests	Good
		R-42 SU1-19	957	Whole element	yes	yes	no	yes	Cladding bend tests	Good
7	Apr 60	R-25 SU1-40	708	Whole element	yes	yes	no	no	Cladding bend tests	Damaged
8	Apr 60	R-31 SU1-17	745	Sections of hanger rod hold down tube	yes	yes	no	no	Microhardness traverse	Damaged
9	Apr 60	R-56 SU1-3		Cladding sections and cotter pin	yes	yes	no	no		
10	Apr 60	R-24 SU1-15	303	Moderator can + Whole element	yes	yes	yes	yes	Cladding bend tests	Damaged

Total Elements Observed in Evaluation

Damaged Elements and Parts	5, of a total of 13 damaged
Undamaged Elements	4, of a total of 30 undamaged
Structural Damage	12 (includes R-31 and R-56)

*These samples were taken, but were of higher radiation intensity than could be handled.

III. DISCUSSION

A. GENERAL

It has been stated, in other documents,[1,4] that the damage to the fuel elements resulted from the blockage of some of the reactor channels by the Tetralin decomposition products. This condition resulted in a temperature rise, high enough to cause the formation and melting of alloys of uranium and the constituents of Type 304 stainless steel. This conclusion as to the cause of the failures was based on the observation of low-melting iron-uranium alloys which had been found at that time (these alloys were of near-eutectic composition, and will be referred to as such).

Since that time, ten hot cell examinations have been conducted (see Table II). The results from these examinations do not show any need for a change in the conclusion reached previously. However, the explanation originally given tends to be over-simplified. This statement is made in light of observations showing two modes of fuel element damage. These facts will be brought out in the discussion and elaborated on briefly.

B. EUTECTIC MELTING

The evidence of the eutectic melting and fuel channel blocking is presented in Figures 7 and 8. Reference to these figures indicates several things. In the case of the fuel elements occupying channel positions R-55 and R-24 (Figures 7 and 8), definite proof of eutectic melting was found by both chemical (Figure 7-p) and metallographic analyses (Figures 7-e and 7-f). In the case of R-55 (Figures 7-a, 7-b, 7-c, and 7-d), the material was found adhering to the cladding and the wire wrap as a "blob". Both the metallographic examination (Figures 7-e and 7-f) and the chemical analysis (Figure 7-p) verified the existence of the proper preportions of these materials to represent the eutectic composition. In the case of R-24 (Figure 8-a), a massive amount of this eutectic material was found, 18 in. below the point of melt-through, in a form suitable for metallographic analysis (Figure 8-f). This metallographic specimen resembled the structure of the eutectic material found in R-55 (Figures 7-e, 7-f, and 8-h-1) and that found in melt-through tests conducted by the SRE program (See Figure 8-h-2). A comparison of the photomicrographs of the cladding taken from both

R-55 and R-24 also indicates that the same characteristic type of cladding "erosion" is found (Figures 7-g and 8-g-1). The diffusion of the iron was toward the uranium, and the interface of this action was relatively straight and easily discernible.

The phase diagram of uranium and iron shows the approximate composition (11 wt % Fe - 89wt % U) and temperature (1337°F) required for this reaction (See Figure 15). The chemical analysis of the "blob" of material indicates the proper proportions for eutectic formation, as seen in Figure 7-p.

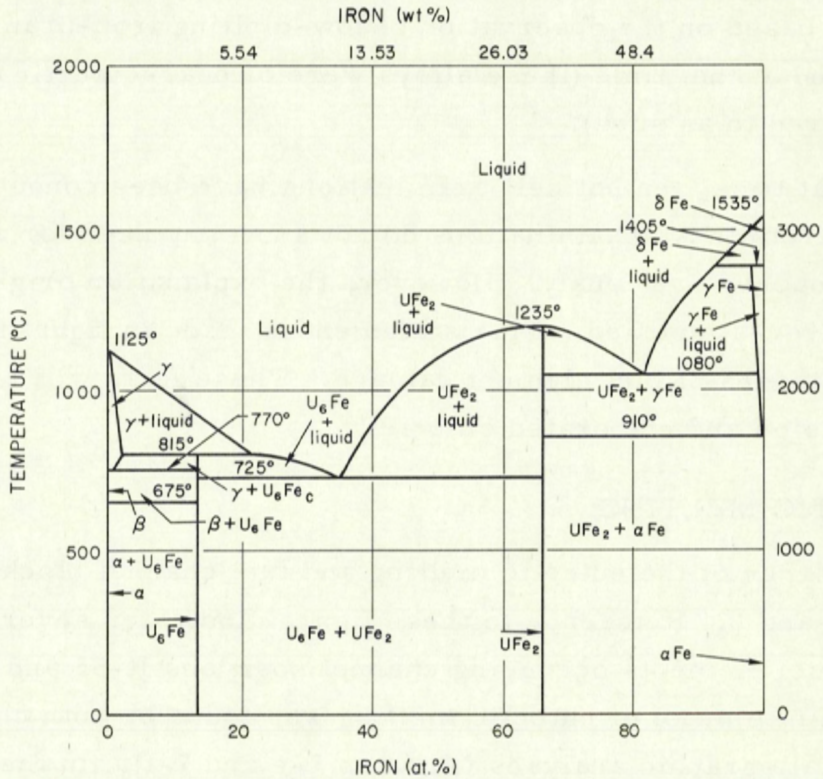

Figure 15. Constitutional Diagram of Uranium-Iron System

It is interesting to note, in Figures 7-h, 7-i, 7-j, 7-k, 7-l, and 7-m, the difference in the resistance of the several metallic fuel materials (U - 1.5 Mo, U - 1.8 Mo, U - 3 Mo, Th - 5.4 U, and U - 2 Zr) contained in element R-55 to damage under these conditions. The thorium indicated practically no effect, as far as irradiation damage was concerned. The U - 2 Zr represented the opposite extreme, where the deterioration was severe, with the metal surface looking much like "coke". It was held together only by the center thermocouple. The dimensional measurements taken on the U - 1.2 Mo and the U - 1.8 Mo (Figure 7-n) indicated that significant erosion of the fuel had taken place, in the order of 0.025 in. from the diameter. The erosion is thought to be a result of the alloying of the cladding and the fuel. However, it should be noted that, in some cases, the slugs represented in the picture were the only slugs recovered in the element (See Figure 7-o).

The temperature of Fuel Element R-55 was measured by two in-fuel thermocouples that operated during all SRE runs, including No. 14. These indicated that, at positions of 15 and 25 in. into the fuel, the temperatures, in the center of the fuel, were high enough (1465°F) to form an iron-uranium eutectic (1340°F) (See Figure 11).

C. FUEL CHANNEL BLOCKAGE

The fuel channel blockage problem is an interesting one. A look at the layout of the reactor face shows the fuel elements that were damaged (See Figure 2). No pattern appears to be present in the failure; damage is random. This would tend to support the fact that blockage occurred, because of the randomness of the damage that might be expected with this condition. Another interesting observation is that the hottest or innermost rings, where the maximum burnup occured (Figure 1), were not affected any more than the others. These are the areas where the maximum swelling or growth would be present, thus accentuating any damage. However, no noticeable effect of this nature was found.

Particular reference is made to the photographs in Figures 8-a, 8-b, 8-c, and 8-d. These show the entire fuel element, as exposed when the process tube was cut longitudinally and removed. It will be noted that five separate areas are visible. Starting from the lowest point, the orifice plate area, Figures 8-d and 8-e show the black sponge-like material present in the channel. Pieces of this material, presumed to be partly hydrocarbon residue from Tetralin decomposition, were removed and tested for solubility. They were insoluble in both room temperature water and after a short-time immersion in amyl alcohol. Subsequent immersion in amyl alcohol, for a extended period, showed some softening and breakup, but not at extensive solution. This is very convincing evidence that a blocking medium was present.

The next area is that of the melted blob, where the melted material solidified (See Figure 8-f). From its relative position, it would appear that the relatively low temperature in the colder area of the fuel element (about 18 in. below the cladding break) caused the melt to solidify. The melt was cast around the entire element, at this point. The cladding adjacent to the solidified eutectic did not show any noticeable erosion or pitting. Metallographic specimens taken of this melt are shown in Figure 8-h-1, and a comparison made with a photomicrograph of an unirradiated specimen of Fe-U eutectic material (See Figure 8-h-2). The similarities are noteworthy. There is some structural modification from the irradiation; however, the same basic microstructure pattern is present. Experience has shown that, where the stainless steel and the uranium reach the eutectic temperature, the Fe-U diffusion forms a sharp interface. Figure 8-g-1 shows the line after the uranium was removed from the cladding by pickling. The relatively straight line seen in this figure is characteristic of the interface reaction. Thus, the conclusion reached, from metallographic evidence, was that the melted material was Fe-U eutectic. The direct chemical analysis of this material was not possible, because of the high nuclear activity.

The third area noted on the fuel element was the area of longitudinal cracks. This is the area from which the material found in the solidified blob originated. The cladding was "eroded", and showed carburization (up to 0.3 to 0.4% carbon) as well as grain boundary effects (Figures 8-g-1, 8-g-2, 8-g-3, 7-g-1 and 7-g-2). The cracks, or openings, were longitudinal in nature and ragged. Pieces of cladding were missing. When the remaining cladding of this area was removed, the slugs inside were still in place. They were eroded, and all of the them had decreased in diameter about 100 mils. All seven of the rods were ruptured longitudinally. When the slugs found in this central area (the area of highest temperature) were measured, the equivalent material was about equal to the mass of the melted blob found about 18 in. below, thus pin pointing the source of the melt. The fourth area is that characterized by radial and diagonal cracks in the cladding, but without the erosion or affected cladding area. The cladding failures in this area were ductile failures, resulting from thermal cycling and expansion of the fuel. This conclusion is reached by comparing the evidence from other irradiated rods (Figures 9-a, 9-b, and 9-c) and from out-of-pile work (Figure 9-d), which shows a similarity in the appearance of the failure. This information, added to the thermal history of Rod R-55, which cycled many times through the α-β phase transformation temperature, strongly indicates thermal cycling as a cause of failure. Area five, the uppermost part of the element, shows clean undamaged rods. When these rods were examined, they were found to be in good condition. All of these observations strongly suggest that intermittent blocking of the fuel element channel took place. This provided the opportunity for eutectic melting and failure of the cladding from the expansion occurring during rapid thermal cycling through the α-β phase transformation. The fuel element from Channel R-24 was the only damaged fuel element completely recovered and examined.

D. THERMAL CYCLING

Several of the fuel elements (R-12, -21, and -25) were found to have splits or cracks in their cladding. Some of these can be seen in Figures 9 and 10. There was no evidence of eutectic melting found associated with these elements. They were nevertheless damaged. The analysis of the temperature data included the checking of the "in-fuel" temperature on the fuel element in Reactor Channel R-55, and the sodium outlet temperature data common to all of the elements in the reactor. A careful check of this information suggested that some temperature anomalies had been experienced, as early as Reactor Run 8. The symptom exhibited can be seen in Figure 11. In the case of Channels 24, 25, and 43, the sodium outlet temperature tended to hunt, or show fluctuation, about the point of average temperature. It was postulated that this indicated that partial or temporary plugging of the reactor channel was taking place at that time. During Run 8, and several times after, in the reactor operating history, the reactor operators were able to correct this hunting condition by jiggling the fuel element, presumably dislodging material from the partially clogged orifice. However, during Run 14, this jiggling was not sufficient to dislodge the plugging material. This plugging is presumed to be a result of the Tetralin leak and the associated decomposition of the hydrocarbons.

Further analysis of the temperature data from the in-fuel thermocouples indicated that the temperatures were cycling up through the range of the α-β phase transformation for uranium (1225°F) A 5% anisotropic volume increase results during a change from the orthorhombic α phase to the tetragonal β phase.

Figure 11-a shows that, in both cases (the 15 in. in-fuel and the 25-in. in-fuel thermocouples), the passage through the transformation temperature had occurred more than 70 times in the 24-hr period on July 23, 1959. The measured period of these cycles is 5 min or less. Since noncontinuous recorders were used, the number of cycles was probably much higher. This would suggest that some

rather high stresses and volume changes resulted from repeated rapid period cycling. A plausible explanation of the temperature cycling of the damaged elements is given in Reference 11.

With this new information concerning the thermal cycling possibility, the literature was examined to see what work had been done on thermal cycling of natural uranium, and particularly with a short-cycle period.[5,6,7,8,9] Generally, the thought expressed was that the cycling influence in-pile would be intermittent, resulting from things such as scrams, or that associated with moving up or down in power. The rapid cycling period had not been considered, because it was thought improbable. The rapid cycling period referred to here is less than 15 min per complete cycle. For this reason, tests were initiated to see what this effect might be. Since the fuel had been assumed to have grown, as a result of irradiation of the material, the available fuel cladding annulus was decreased from 0.010 to 0.003 in. There was no original SRE fuel available; therefore, depleted uranium metal with a similar fabrication treatment was substituted. This material was turned from 1.125 in. in diameter to 0.784 in. in diameter, and placed in a section of the standard SRE 0.010-in. wall by 0.790-in. ID tubing. Since facilities for the use of sodium were not available, an inert gas bond of helium was substituted in the capsule. It was then placed in the thermal cycling furnace, set for 5 min at temperature and then 5 min to cool off through the temperature range of 900 to 1300°F. The heating medium was a neutral heat treating salt bath.

Both capsules failed in less than 24 hr, with a total of between 275 and 300 cycles (See Figure 9-d), thus reinforcing the idea that repeated rapid cycling through the α-β phase transformation temperature (1225°F) could be responsible for fuel cladding damage. The capsules for this test utilized in-fuel thermocouples for controlling temperature. The cladding failures found on the damaged fuel elements appeared to be similar to the cladding failures encountered in the thermal cycling tests.

The bark-like appearance of the fuel shown in Figure 10-f is unlike the normal metal failure expected under these conditions. It strongly resembles the external surface present when burning or strong overheating of a metal takes place. This occurs where the external surface is actually cooler than the internal volume, or where an oxide layer is built up which strengthens the surface layer of metal. Thus, when the internal pressure created by the thermal expansion takes place, it puts the exterior surface in tension. When the stress is high enough to cause rupture, the bark-like cracking takes place. Another source of external strain is the wire wrap. In examining the unalloyed uranium that showed this bark-like appearance (Figures 10-b, 10-c, 10-d, 10-g, and 10-f), it appears to have occurred where the cladding was absent; presumably, the cladding had deteriorated from the other causative factors.

The damaged rods shown in Figure 10 show this effect, that may support the thesis of the growth due to fast period thermal cycling. These slugs are out of round, and the wire wrap is imbedded in some of them.

The marks on the slugs indicate deformation that resulted from external strain caused by the wire wrap (Figures 10-b, 10-c, and 10-d). The wire wrap is 0.090 in. in diameter, and winds in a helix on about a 10-in. pitch. This tends to be a very rigid member, relatively speaking. When the fuel expands, the wire wrap causes the fuel slug to deform. A close look at the deformation indicates that (1) the deformation took place where the cladding did not provide restraint, and (2) the deformation tended to be more prevalent on the side away from the wire wrap, or where the point of greatest tension would be present. The side near the wire wrap tends to show crushing or bearing and some cracking, but not to the same extent as on the far side. Once this cracking has taken place, the coolant sodium tends to be absorbed in the cracks and accentuates the condition, by not allowing the cracks to close completely. It is suggested that such a condition would also be accentuated by thermal cycling, once the cladding had been split open. To verify this idea experimentally, a test was run in which 0.090-in. diameter stainless steel wire wrap was placed on three SRE-type test capsules. The capsules were subjected to internal pressure bursting tests, at temperatures of 1000°F. The results of these tests indicated that the wire wrap is considerably stronger than the cladding (Figure 9-e). Therefore, the cladding and/or fuel that would be inside of them would be deformed, as it attempted to expand, because the wire wrap would not elongate appreciably. It would then appear reasonable to assume that the wire wrap has an influence on the damage of the cladding when a thermal cycling takes place. This again is evidenced by the deformation of these slugs and the shear failures of the cladding, as seen in some of the pictures of Figure 12.

The support for the thesis of the thermal cycling is that a vast amount of swelling or growth took place, and that the deformations were visible.

These phenomena are not independent, but are the result of interactions of all the things that were present, such as the fuel channel blocking, thermal cycling, wire wrap restraint, and eutectic melting.

Figure 12 suggests that the cladding has been stretched beyond its limit and failed. This is the kind of failure associated with the thermal cycling. The qualitative bend tests of the cladding did not indicate significant changes in ductility that would account for a brittle failure. The end view of the slugs in Figure 12 shows the bark-like appearance of the fuel, with the white material absorbed in the cracks. This appearance is not typical of metal, it is more suggestive of ceramic or coke.

Reference to Figure 12 also shows several transverse sections of fuel slugs that were taken from Fuel Element R-55. Figures 12-d-1 through 12-d-6 show sections from unalloyed uranium. Some voids were noted, in the central part of the metal, that presumably could be the consolidation of the fission gas within the uranium slug. The second set of these specimens (Figures 12-e-1 and 12-e-2) shows the Th - 5.4 wt % U that was subjected to the same conditions. It has no indication of the void formation. This is evidence of the greater stability of the Th-U to the conditions encountered in this reactor.

E. EXAMINATION OF UNDAMAGED ELEMENTS

Figure 10-h shows an undamaged fuel element taken from Reactor Channel R-45. This was a reference fuel element that had been followed, throughout the entire reactor operating history, by nondestructive examinations. After Run 14, it was selected for comparison with those elements that had been damaged. Figure 10 shows a composite of the undamaged fuel element, closeups of the slugs (Figures 10-j and 10-k), and measurements made of the entire element (Figures 10-l and 10-m). There was nothing abnormal about this element in the data reported before or after the final reactor run. For further information, the rods were opened, and slugs from the top, middle, and bottom of the rod were selected for examination. They showed swelling, but only that amount expected from the SRE Core I burnup.[3]

There were four additional undamaged fuel elements that were examined, in conjunction with the long-term reactivity program. Elements of differing burnups (and hence, differing lengths of residence in the reactor) were selected. All of then had been present in the reactor during Run 14 (See Table II). These rods had a thorough visual check, as part of the gamma-scanning procedure. In this procedure, the rods were viewed, over their full length at three radial positions, to obtain burnup profiles. The examination showed them to be completely intact, and nothing abnormal was found in the examination of these rods.

F. STRUCTURAL DAMAGE

Another fundamental question to be answered by this investigation was whether or not there was evidence of significant structural damage, on either the fuel element cladding or any of the associated fuel element hardware, resulting from the Tetralin leakage and/or the nitrogen purge introduced as part of the stripping operation.

The Tetralin leakage placed in the sodium coolant system a large quantity of decomposition products (primarily carbon). This presented the possibility of massive carburization of the steel cladding. The carburization, in turn, could have resulted in embrittlement of the stainless steel. An initial conclusion along this line was reached, based on a piece of the fuel element cladding from R-55 (Figure 7-g-2) that dropped from the fuel handling cask. On this same piece of cladding was found a "blob" of eutectic material (Figure 7-e). In all of the subsequent examinations of cladding materials, by qualitative bend tests, metallographic tests, and chemical analysis, no evidence has been presented or found which shows that massive carburization or any surface deterioration had taken place. These pieces of cladding and hardware have been selected from positions over the entire length of the fuel element, including the upper hardware or the hanger rod holddown tube. The only place where evidence of surface deterioration was seen was adjacent to the melt-through area (Figure 7-g-2). Thus, the conclusion has been drawn that no damage was done to the cladding or structural materials by the Tetralin or nitrogen purge, except where the melt-through conditions from the fuel channel blockage resulted in an abnormally high temperature.

Pieces from the hanger rod holddown tube from the fuel element in Reactor Position R-31 were taken from two locations, one immersed in sodium (at reactor outlet temperature), the other from the vapor phase above the sodium pool. Neither of these pieces showed any effect from carburization or nitriding. There was the effect of sensitization* that accompanies the heating of Type 304 stainless steel. This effect was evident only in the case of the immersed liquid location, and not in the sample that had been taken from the location in the vapor phase (see Figures 13-c-1 and 13-c-2).

A microhardness traverse (Figure 13-d) was made on the piece of tube from Fuel Element R-31 present in the sodium pool. The microhardness traverse showed higher hardness in the outer third of the tube wall than for the center third. This coring effect was a result of the extended exposure at temperature. The hanger rod tube has a section thickness three times greater than the cladding; therefore, the penetration of the sensitized structure was somewhat less than that of the whole section. The presence of carbon in the grain boundaries increased the hardness reading perceptibly.

A check on the condition of the fuel element hardware, prior to Run 14, was of interest. By chance, an element that had been in the reactor during its entire operating history had been damaged in the wash cell, after completion of Run 13, thus causing it to be left out of the reactor during Run 14. Part of this element was extracted from the wash cell and examined. The cladding from this element, shown in Figure 13-a-1, indicates a sensitized structure; however, it does not show any surface deterioration or attack. There is no evidence that this cladding was significantly different from that exposed during Run 14. A specimen was prepared from a cotter pin, made of Type 304 stainless steel, taken from the element damaged in the wash cell (Figure 13-b). The sensitized structure was present, but no attack was in evidence. A comparison was made between the microstructure of the irradiated cladding from this element (Figure 13-a-2) and "as-received" material (Figure 13-a-4). The difference in structure was insignificant.

---

*Sensitization – The precipitation of the residual carbon in the grain boundaries, associated with and resulting from soaking stainless steels at high temperatures. This condition is seen by metallographic examination.

G. MISCELLANEOUS

In the attempt to withdraw all elements from the reactor, after the shutdown from Run 14, considerable lifting effort was employed by the crane in the SRE high bay area. It is believed that the effect of this withdrawal force could, or would, alter the character of the indicated damage seen on the cladding. During removal, all of the elements (including R-24, the element recovered from the moderator can) were subjected to this force. Therefore, there still remains the possibility that the mode of failure or damage was masked. In view of the fact that not all of the elements could be thoroughly examined, this factor cannot be adequately assessed.

Early in this investigation, a suggestion was made that the cladding might be failing, as a result of irradiation damage. This suggestion was made at a time when no real pattern of explanation was available. The completion of the examination of R-24 placed a different light on the entire investigation. Though the suggestion of the radiation damage was sound and reasonable, there does not seem to be any evidence to support it effectively, as a major part of the fuel damage mechanism.

IV. CONCLUSIONS

Based on the investigative work on the metallurgical nature of the fuel element damage, the following conclusions have been drawn:

The evidence points to a gross blocking of the fuel element channel, that resulted in a rapid rise in fuel temperature. Hence, a temperature, high enough to support the iron-uranium eutectic formation, resulted in the cladding failure.

The blocking of the channels was a result of the formation of carbon from Tetralin coolant decomposition, sodium oxide, and/or other foreign materials in the coolant.

There was extensive thermal cycling of the damaged fuel elements, thought to be a result of the intermittent blocking of the fuel element process tube channel and changes in reactor power.

The rapid and repeated thermal cycling through the α-β phase transformation temperatures caused growth of the uranium slugs and failure of the fuel element cladding exclusive of the eutectic reaction considered elsewhere.

The wire wrap had a restraining action upon the swelling of the fuel slugs.

There is no evidence to suggest that the stainless steel cladding or upper hardware was affected by either the nitrogen purge or the carbon in the sodium coolant.

There was no significant metallurgical difference between cladding materials present in the reactor, prior to Run No. 14, and those present during Run No. 14.

The stainless steel structural members and cladding tend to show a sensitization of the material, resulting from time at temperature. However, this material has not shown any significant decrease in physical properties, or a decrease in the ability of the material to perform its intended function, judged by qualitative tests.

The cladding has shown itself to be compatible with its environment, and has shown no effect or indication of deterioration. The notable exception to this statement is the cladding immediately adjacent to the melt area. Significant attack did take place, at this point, and is presumed to be associated with melt-through.

REFERENCES

1. A. A. Jarret *et al.*, "SRE Fuel Element Damage, An Interim Report," NAA-SR-4488 (November 30, 1959)
2. B. R. Hayward and J. W. Walter, "SRE Experimental Fuel Program (Interim Report)," NAA-SR-3456 (October 15, 1959)
3. J. L. Ballif *et al.*, "SRE Fuel Irradiation Experience," NAA-SR-3887 (September 1959)
4. R. W. Dickinson, "Coolant Block Damages SRE Fuel," Nucleonics 18, No. 1 (January 1960) p 107
5. H. M. Finniston and J. P. Howe, *Metallurgy and Fuels* (McGraw Hill Publishing Co., New York, N.Y., 1956) p 120
6. A. N. Holden, *Physical Metallurgy of Uranium* (Addison Wesley Publishing Co., Inc., Reading, Mass., September 1958) p 192
7. W. D. Wilkinson and W. F. Murphy, *Nuclear Reactor Metallurgy* (D. Van Nostrand Inc., Princeton, N. J., 1958) p 108
8. J. R. Dietrich and W. H. Zinn, *Solid Fuel Reactors* (Addison Wesley Publishing Co., Inc., Reading, Mass., 1958) p 223
9. B. R. Hayward, "Dimensional Changes Resulting from Alpha-Beta Thermal Cycling of Uranium and Uranium Alloys, "NAA-SR-1434 (March 15, 1956)
10. R. S. Neymark, "Rate of Alloying of Uranium Alloys with Stainless Steel," NAA-SR-3278 (June 1, 1960)
11. R. L. Ashley *et al.*, "SRE Fuel Element Damage, Final Report." NAA-SR-4488 Suppl. (June 30, 1961)